Challenges in seismic hazard assessment

Analyses of ground motion modelling and seismotectonic sources

Mathilde Bøttger Sørensen

Dissertation for the degree philosophiae doctor (PhD)

at the University of Bergen

March 2006

Preface

The work presented in this thesis was initiated in February 2003 when I was enrolled with the Ph.D. program of the University of Bergen (UiB). The thesis consists of two parts. The first part is a summary of the work I have done during my Ph.D. studies, including some background information and a discussion on future challenges within the described topics. The second part, which is the main outcome of my studies, is a collection of seven research papers, which are all currently either in review or accepted for publication in international journals.

The focus of this thesis is on seismic hazard in the broadest sense of the term, spanning from seismotectonic studies to direct hazard assessments. Seismic hazard has been assessed in three main regions, taking into account the seismicity level in the studied region when choosing which methodology to apply. The papers can be divided into two main groups, reflecting my involvement in two separate research projects. The first group of papers deals with seismic hazard and ground motion modelling in high-seismicity areas (the Marmara Sea and the Sumatra regions), and has been completed mainly under the EC project RELIEF (EVG1-CT-2002-00069). The second group has been completed as part of my involvement with the seismo group of Department of Earth Science, University of Bergen and deals with seismotectonic studies of selected areas in Norway. The work on the two parts has been carried out in parallel during the last three years.

My main contribution to the work of paper 1 ("Ground motion scaling in the Marmara region, Turkey") was during a one-month visit at INGV, Rome, where I worked on a preliminary dataset, mainly in collaboration with Aybige Akinci. Unfortunately the dataset was insufficient to obtain stable results. The study was finalized later on when complementary data were available. I have not been directly involved in this phase of the work. I estimate my contribution to the paper to be approximately 10%.

The work of paper 2 ("Sensitivity of ground motion simulations to earthquake source parameters: a case study for Istanbul, Turkey") has been developing over a long time with many foregoing tests of the ground motion simulation methodology. There has been collaboration with Nelson Pulido from National Research Institute for Earth Science and Disaster Prevention, Earthquake Disaster Mitigation Research Center (NIED - EDM), Kobe, Japan, mainly regarding technical issues with respect to the simulations and through discussions on how to present the results. The majority of the scenario computations were completed during the summer of 2005. I estimate my contribution to the paper to be approximately 90%.

Paper 3 ("Local site effects in Ataköy, Istanbul, Turkey, due to a future large earthquake in the Marmara Sea") was written as a result of a close collaboration mainly between three different groups. Ivo Oprsal and Martin Mai from ETHZ, Zurich, Switzerland, were involved in the 3D FD computation part of the study. This collaboration included a one-week workshop in Zurich in March 2004, where we set up the framework for the computations with main focus on the input velocity model. The 3D FD computations were performed by Ivo Oprsal. The 1D modelling of ambient noise was performed by Sylvette Bonnefoy-Claudet of LGIT, Université Joseph Fourier, Grenoble, France. The microtremor data used for H/V spectral ratio analysis were collected during a 10-day field survey in Istanbul in October 2003. My main contribution to the paper has been in data collection and processing of microtremor data, in building the 3D input velocity model for the 3D FD computations and in the writing process, collecting and synthesizing the results. I estimate my contribution to be approximately 60%.

The study described in paper 4 ("Simulated strong ground motions for the great M 9.3 Sumatra-Andaman earthquake of December 26, 2004") was initiated following the December 26, 2004 Sumatra-Andaman earthquake. The motivation for this study was two-fold. Firstly, while there had been an intense focus on the tsunami effects and source model following the earthquake, the issue of ground shaking had not been much discussed. Secondly, we were interested in testing the performance of the

ground motion simulation methodology of Pulido et al. (2004) in modelling such a large event. Again, we collaborated with Nelson Pulido, both regarding the technical issues and in discussing the input source model. I estimate my contribution to be approximately 80%.

The study of paper 5 ("Tectonic processes in the Jan Mayen Fracture Zone based on earthquake occurrence and bathymetry") was motivated by the April 14, 2004 Jan Mayen earthquake. The main collaboration was with Lars Ottemöller from BGS, Edinburgh, UK, who performed the waveform cross-correlations and relocated the aftershocks using JHD. My main involvement in the work was in the manual relocation of aftershocks and in the coulomb stress modelling. I estimate my contribution to be approximately 65%.

Before the initiation of paper 6 ("Seismotectonics of Skagerrak") there had long been a discussion within the seismo group of UiB that we wanted to focus on the Skagerrak area in the future. Data from the Danish stations were collected over a long time until we obtained contact with Jan-Erik Lie of RWE Dea Oslo, Norway. He offered to provide interpreted seismic data to be used in a seismotectonic study of Skagerrak. I estimate my contribution to the paper to be approximately 85%.

The Rana region was another area, which we had long been discussing to study in more detail. This had lead to the installation of the temporary field stations STOK1 and STOK2, in which I was involved during a field trip in July 2005. Following, we were contacted by Steven Gibbons from NORSAR who suggested a collaboration regarding these earthquakes (paper 7, "The detection and location of low magnitude earthquakes in northern Norway using multi-channel waveform correlation"). All work regarding cross-correlation of recorded data has been carried out by Steven Gibbons, whereas my main involvement has been in extraction of data and earthquake location. I estimate my contribution to be approximately 35%.

Mathilde Bøttger Sørensen,
March 2006

Abstract

Seismic hazard assessment has an important societal impact in describing levels of ground motions to be expected in a given region in the future. Challenges in seismic hazard assessment are closely associated with the fact that different regions, due to their differences in seismotectonics setting (and hence in earthquake occurrence) as well as socioeconomic conditions, require different and innovative approaches. One of the most important aspects in this regard is the seismicity level and the pre-existing knowledge about seismotectonics and fault behaviour in the region. The present thesis focuses on seismic hazard in three regions of very different tectonics in which different approaches for seismic hazard assessment were needed. In seismically active regions, standard probabilistic and deterministic approaches can be followed in assessing the hazard provided that the seismotectonic and geological information is available. In regions of low seismicity, this information is often incomplete and it may be necessary to start by studying in more detail the seismotectonic processes giving rise to the seismic hazard. The Marmara Sea and Sumatra regions are the main geographical areas where challenges in high seismicity areas are addressed. For addressing the seismic hazard assessment in low seismicity areas, the approach was to focus on the seismotectonic source characterization in various locations in Norway and adjacent areas.

The Marmara Sea region is under a significant seismic hazard due to the short distance to the North Anatolian Fault which is believed to be close to rupture. This region is well studied in terms of tectonics and fault properties. However, the attenuation properties of the crust in the region have been uncertain. A new attenuation relation is established for the region, based on regressions performed on the background seismicity (paper 1). The obtained relation shows good agreement with previously used relations. Due to the increased level of knowledge about the active faults in the Marmara Sea, scenario based ground motion modelling provides a reliable estimate of the seismic hazard due to a future large earthquake. The

predictive nature of such computations leads to uncertainties in the input parameters, the effect of which has not been well known previously. A study of the effect of varying input source and attenuation parameters (paper 2) shows that rise time, rupture velocity, stress drop and rupture initiation point are the most significant parameters in terms of ground motion level. The effect of parameters and the variability of ground motion are strongly frequency dependent. Another factor leading to uncertainties in simulated ground motion is that most simulations are performed at bedrock level without taking possible site amplifications into account. This latter problem is addressed in a separate study in the Ataköy area, SW Istanbul (paper 3), which shows that site amplification is significant over the whole area with amplification up to a factor of 2.

The December 26, 2004 Sumatra-Andaman earthquake left many unanswered questions regarding the importance of ground shaking in the observed damage and, more generally, the nature of ground shaking caused by very large earthquakes. To address these issues, the event is modelled in terms of ground motion to see the effect of ground shaking in the regions near the fault rupture (paper 4). Results show that ground shaking was significant in northern Sumatra and the neighbouring islands and set bounds on the ground motion to be expected from such large events.

The low seismicity in Norway and the surrounding areas makes it difficult to understand the relationship between the tectonics (active faults) and the earthquake activity. In order to improve this, three regions of significant seismic activity have been chosen for further seismotectonic investigations. The Jan Mayen region is, with its location on the mid-Atlantic ridge, the seismically most active region in Norway. Despite this fact, very little was previously known with respect to active fault structures. Locations of a M=6.0 earthquake and its aftershocks, combined with a detailed bathymetry, have provided new evidence about active tectonic structures in the region (paper 5). It is shown that major strike-slip earthquakes occur along the Koksneset fault, which seems to be the dominant structure in the Jan Mayen Fracture Zone. In addition, NE-SW oriented normal or oblique normal faults are being

reactivated in the Jan Mayen Platform as a result of the deformation along the Koksneset fault.

Deformation along the plate boundaries is significantly different from intraplate deformation. In this sense, the tectonic setting of Skagerrak situated in a basin within the Eurasian Plate is very different from Jan Mayen. This is reflected in the seismicity, which is much lower than for Jan Mayen but still high in comparison to other regions in Norway. Most earthquakes here have magnitudes less than 3, which in combination with the offshore location makes earthquake location challenging. Increased station coverage during the recent years has improved the location capabilities and the combination of relocated seismicity with reinterpreted seismic profiles and gravity and magnetic anomaly data has provided new clues about the origin of the Skagerrak seismicity (paper 6). A previously unknown graben structure, the Langust fault zone, is found at a location coinciding with the location of the local seismicity. This structure is believed to be the source of a large part of the Skagerrak earthquakes. In addition, activity seems to be present along the Sorgenfri-Tornquist Zone, as it is also the case further southeast in Kattegat.

The Rana region in northern Norway is unique in the sense that several earthquake swarms have been registered here earlier. The installation of two temporary stations in this active region has provided high-quality recordings of events down to magnitude less than 0.5. In addition to providing new information about the seismotectonics in the region, these events have been used as ground truth in calibrating event detection based on waveform correlation (paper 7).

In combination, the presented studies address some of the challenges associated with seismic hazard assessment, and can hopefully serve as a basis for further investigations in the future.

Acknowledgements

I am grateful to a large number of people who have contributed to this thesis either through direct collaboration or through supporting me on a professional or personal level.

First I want to thank my supervisors Kuvvet Atakan and Jens Havskov for their supervision and support, for the enlightening discussions and for providing an excellent environment for their students. I also wish to thank my co-authors, who have provided important contributions to the work presented. I am grateful to my colleagues in the seismo group at Department of Earth Science (IFG) (Annelise Kjærgaard, Helge Johnsen, Jose Å. Ojeda, Terje Utheim and Berit Marie Storheim) who have integrated me in the group and been supportive of my work. And also to the IT group and the administration of IFG who helped me solve many practical issues over the years.

The work regarding seismic hazard is carried out as part of the EC project RELIEF (EVG1-CT-2002-00069) and I wish to thank all the RELIEF partners for fruitful discussions and many fun hours during field work, workshops, meetings etc. In addition, our colleagues at the KOERI (Eser Durukal, Yasin Fahjan, Gülüm Birgoren, Oguz Özel, Karin Sesetyan, Mustafa Erdik and Atilla Ansal) have been a great help and provided a pleasant environment during my visits in Istanbul over autumn 2005.

The work on seismotectonics in Norway has been completed under the NNSN. I appreciate the discussions and help of colleagues from NORSAR (Conrad Lindholm, Hilmar Bungum, Steven Gibbons and Berit Paulsen) and from GEUS in Copenhagen (Søren Gregersen, Tine B. Larsen, Peter Voss and Martin Glendrup). I also want to thank IFG (and especially director Olav Eldholm) for providing additional funding for the last months of my work.

The present thesis summary benefited from comments and suggestions from my supervisors and from Line P. Jensen, Karleen Black and Aleksandre Kandilarov.

I wish to thank all my dear friends without whom the last years would not have been the same. This goes first for my faithful friends home in Denmark who kept contact, visited me in Bergen and always had time to see me when I stopped by. Especially I would like to mention Portvinsklubben (Line P. Jensen, Niels Christensen, Mette Andersen, (Kristoffer) Kreuff Haldrup, Karsten Scheibye-Knudsen, Mads Raben, Stine West, Jesper Q. Thomassen and Jan Erik Revsbech), Kernetøserne (Line P. Jensen, Mette Andersen, Janne R.T. Banke, Anneline Carlsen, Marie Timm and Veronica Jacobsen) and my dear old friend Eva Mondrup. During my time in Norway I have met many great people. Thank you to all my old neighbours in Fantoft and to the other people I met here, especially to Carolin A. Rebernig, Eva Kraus, Carol Jones, Meinrad Pohl, Maria Foged, Christian Himmelhuber and Wladimir Vaca. And last but not least to the other students in the seismo group who have helped me throughout my work and been good friends. Here I especially want to mention Zoya Zarifi, Mohammed Raaesi, Tarek Kebeasy, Margaret Wiggins Grandison, Alexandre Kandilarov, Julia Schinkel, Louise Bjerrum, Hlompo Malephane and Karleen Black

At the end I wish to thank my family. Thank you to my parents Bente and Holger Bøttger and my sister Bolette Bøttger for all their support, for letting me move to Norway and for always letting me feel I have a place to come home to. Also thanks to my grandmother Inge Søholm who has followed me with great interest, and to my aunt and uncle, Åge and Mette Sørensen, who have always been a great inspiration for me.

List of publications

Paper 1: Akinci, A., Malagnini, L., Herrmann, R.B., Gok, R. and Sørensen, M.B. (**accepted**). Ground motion scaling in the Marmara region, Turkey, accepted for publication in *Geophysical Journal International*.

Paper 2: Sørensen, M.B., Atakan, K. and Pulido, N. (in review). Sensitivity of ground motion simulations to earthquake source parameters: a case study for Istanbul, Turkey, submitted to *Bulletin of the Seismological Society of America*.

Paper 3: Sørensen, M.B., Oprsal, I., Bonnefoy-Claudet, S., Atakan, K., Mai, P.M., Pulido, N. and Yalciner, C. (**accepted**). Local site effects in Ataköy, Istanbul, Turkey, due to a future large earthquake in the Marmara Sea, accepted for publication in *Geophysical Journal International*.

Paper 4: Sørensen, M.B., Atakan, K. and Pulido, N. (**accepted**). Simulated strong ground motions for the great M 9.3 Sumatra-Andaman earthquake of December 26, 2004, accepted for publication in *Bulletin of the Seismological Society of America*.

Paper 5: Sørensen, M.B., Ottemöller, L., Havskov, J., Atakan, K., Hellevang, B. and Pedersen, R.B. (in review). Tectonic processes in the Jan Mayen Fracture Zone based on earthquake occurrence and bathymetry, submitted to *Bulletin of the Seismological Society of America*.

Paper 6: Sørensen, M.B., Lie, J.-E., Atakan, K. and Havskov, J. (in review). Seismotectonics of Skagerrak, submitted to *Tectonophysics*.

Paper 7: Gibbons, S.J., Sørensen, M.B., Harris, D.B. and Ringdal, F. (in review). The detection and location of low magnitude earthquakes in northern Norway using multi-channel waveform correlation, submitted to *Physics of the Earth and Planetary Interiors*.

Contents

Part I: Summary

1. Introduction

Earthquake hazard and its relationship to risk, as well as the awareness of local populations to the earthquake phenomenon vary significantly around the world. In some regions, like Scandinavia, common perception is that earthquakes are mainly an exotic phenomenon occasionally causing disasters in far-away places. On the other hand, in places like Japan, Chile or Turkey, earthquakes are part of people's everyday life. In areas of high seismicity, most earthquakes are small and cause no damage, but occasionally disastrous events are reminders of the importance of earthquake hazard and force the local authorities to take measures in earthquake preparedness and risk mitigation. Over the years, the desire to provide tools for earthquake risk mitigation, perhaps with the ultimate goal of earthquake prediction, has led to the development of seismic hazard and risk assessment as important fields in seismology. The presented work in this thesis focuses on various aspects of seismic hazard assessment, whereas the coupling to seismic risk is only discussed briefly for a few cases.

1.1 State-of-the-art of seismic hazard assessment

The main aim of any seismic hazard assessment is to, in some way, quantify the level of ground shaking which can be expected in a given region within a given time. This is naturally dependent on the seismic activity in the region, but also on factors such as the time elapsed since the previous large earthquake and the distance to large faults. Traditionally, probabilistic methodologies have been applied for assessment of seismic hazard, originally based on poissonian earthquake occurrence. With the recent improvements achieved in understanding the behaviour of seismic sources, complicated recurrence models (e.g. renewal models) are now being implemented, taking into account the time elapsed since the previous large earthquake. More recently, due to the availability of more detailed information on the deformational processes involved in an earthquake rupture, deterministic hazard assessment has become more popular through ground motion modelling.

Once the hazard level is known, the next step is to combine with the vulnerability of the built environment in the region to assess the seismic risk. Here it is important to note that the risk is not necessarily proportional to the seismic hazard. It is possible to have regions with high seismic hazard but low seismic risk in cases where there is no or scarce population and structures vulnerable to earthquake loads. On the other hand, regions where structures are vulnerable can be under a significant seismic risk even if the seismic hazard is limited in terms of the expected ground motion levels. The vulnerability of a given region is a complex function of a variety of parameters, which requires integration of several disciplines and is beyond the capacity of seismology. The implications of hazard results in engineering practice and in assessing the risk should however always be kept in mind when working with seismic hazard assessment. For these reasons, the main focus of the present work is on seismic hazard assessment. Implications of the results are discussed in terms of their engineering significance without going into the problem of vulnerability and risk.

The methodology to be applied for hazard assessment in a given region depends on the level of knowledge about the seismicity and the deformational processes in the region. The seismic activity level and potential earthquake sources are important input parameters in all seismic hazard assessments, and if these are not well known, focus should be on such issues. In most active plate boundaries in populated areas, there is a good knowledge on earthquake sources and the frequency of earthquake occurrence, but for plate boundaries in unpopulated areas, this knowledge can be limited. Similarly, in intraplate regions the seismic cycle becomes much longer, which implies that the time of observation needed to obtain a complete picture of the seismicity increases. A classical example here is the 1811-1812 New Madrid, Missouri earthquake sequence. During a two-month period, three earthquakes of magnitudes larger than ~8.0 hit within the stable eastern US (e.g. Lay and Wallace, 1995). The long recurrence times associated with such large intraplate events implies that these events can occur in regions previously thought to be seismically quiet.

In places where the seismicity is well known (i.e. with a sufficient rate of deformation that the seismic cycle is short enough to be observed within the instrumental period), probabilistic methods can be applied for assessment of the seismic hazard. In such studies, the earthquake occurrence is handled statistically and combined with attenuation curves describing the fall-off of the ground motion with distance. If more detailed information is available about individual seismic sources and the deformational processes in the region including strain accumulation, fault behaviour and segmentation, and fault parameters, deterministic hazard assessment can provide a very detailed picture of the seismic hazard. Here, the dimensions of the study area also play a role in that e.g. nation-wide hazard assessment is usually forced to be based on probabilistic methodologies since the hazard on this scale is a combination of contributions of several sources.

Over the last years, there has been an increase in the knowledge about active faults and their rupture properties, leading to increased attention to the deterministic seismic hazard assessment methodologies. However, probabilistic methods are still popular, especially in less studied regions and for large-scale regional studies. Even though it is uncertain whether short-term earthquake prediction will ever be possible in all regions, many efforts aim at some level of prediction. One example here is the California earthquake forecast maps available online from the U.S. Geological Survey, which are updated daily giving the probability of shaking with MMI intensity VI or more (Gerstenberger et al., 2004). In Japan, discussions are towards early warning efforts through intensive monitoring (e.g. the KIKnet of 675 stations). Here, the aim is that early recordings of ground motion at stations close to the rupturing fault can be compared to modelled scenario ground motion to issue early warnings limited to areas expected to be affected by the earthquake (Kiyoshi Suyehiro, pers. comm. 2005). Global seismic hazard was assessed during the GSHAP project, which was run as part of the International Lithosphere Program in 1992-1999 (GSHAP, 1999). The outcome of this project was a freely available global seismic hazard map. A step towards more global efforts and coordination of the hazard assessment is taken through the openSHA (www.opensha.org) project. This project aims towards an

open-source computational infrastructure for seismic hazard assessment, combining different disciplines (seismology, geology, engineering etc.). Models can be plugged into the system via the internet and the output provides great flexibility to the end user in terms of ground motion measure.

1.2 Addressing the challenges in seismic hazard assessment

In the present thesis, efforts have been directed towards studying different regions of both low and high seismicity, using different methodologies depending upon the existing level of knowledge. For the high-seismicity regions, the main focus is on estimating the seismic hazard and providing tools for mitigating the associated risk. On the other hand, in areas of low seismicity, we have addressed the problem by studying and improving the knowledge of the earthquake phenomenon and regional seismotectonics. The geographical focus has been on the Marmara Sea region in NW Turkey, the area of the 2004 Sumatra-Andaman earthquake and three different regions of significant seismicity in Norway, which in general lies in a low-seismicity region.

In the Marmara Sea area, the main concern has been assessing the earthquake hazard in the city of Istanbul associated with a future large earthquake occurring along the western part of the North Anatolian Fault (NAF). The high probability of a large earthquake near this megacity of more that 12 million inhabitants implies a significant seismic risk in the region. Regional attenuation relations have previously been lacking here, and therefore a new attenuation relation is established for the region based on regression of small earthquakes (paper 1). Due to previous intensive studies of the regional tectonics and historical earthquakes, ground motion simulations for large scenario earthquakes can provide hazard estimates of much more direct use for risk mitigation than the probabilistic approaches. One remaining issue in this respect is the effect of varying input parameters on the simulated ground motion. We focus on these uncertainties associated with the simulations and on the

effect of varying the input parameters on the resulting hazard levels (paper 2). Until now, all ground motion simulations in the area have been performed at bedrock level. Local geology plays an important role in amplification of ground motion for parts of the Istanbul area, and should be taken into account. The Ataköy area in southwestern Istanbul has been the target of a study on local site effects (paper 3). Here, site effects are estimated following three different approaches and a first estimate of amplification of strong ground motion is obtained.

In addition to the Marmara Sea region, one paper focuses on the Sumatra region and the December 26, 2004 Sumatra-Andaman earthquake (paper 4). This study was initiated after the 2004 earthquake and focuses on modelling the ground motion caused by the event. The motivation came from the lack of strong motion recordings after the earthquake and an interest in estimating the level of damage caused by ground shaking in northern Sumatra before the tsunami hit. Additionally, it was desired to investigate further the distribution of ground motion in case of very large earthquakes.

Most of the Norwegian area is located within the Eurasian plate and therefore the seismicity is relatively low. Despite this, a number of locations have increased seismicity, and three of these have been studied in this thesis. Basic questions about seismicity and earthquake occurrence still need to be answered, and therefore the main focus has been on the seismotectonics of the three areas. The most active area on Norwegian territory is around the Jan Mayen island, situated on the mid-Atlantic ridge. This area is located on an active plate boundary, but the remote location has made previous studies uncertain and association of earthquakes to specific fault structures has not been possible. The availability of recently collected bathymetric data for the region and high-quality recordings from a local seismic network has made such an association possible for the first time (paper 5). Another active area is under the Skagerrak Sea between Norway and Denmark. Here, it has long been known that the activity is high, but the source has been unknown. The combination of Norwegian and Danish earthquake recordings provides much new information about

the earthquake occurrences and new interpretations of seismic data provide clues about the origin of earthquake activity (paper 6). The third region studied is the Rana region, northern Norway. This has been known to be an unusually active area with a high seismicity level and numerous earthquake swarms. Recordings of the many small earthquakes occurring within very limited areas make it possible to test detection techniques based on waveform correlation (paper 7).

2. Seismic hazard and ground motion modelling in high-risk areas

This section describes seismic hazard assessment in two regions known to be affected by significant seismicity; the Marmara Sea and the Sumatra regions. The main focus is on the Marmara Sea region in NW Turkey, where three papers are dedicated to several aspects of seismic hazard in the area. This region has been subject to numerous studies of tectonics, seismicity and probabilistic seismic hazard, and the available information makes deterministic seismic hazard assessment possible. Issues that still need to be resolved in the region include the attenuation of seismic waves, the uncertainties associated with input source parameters in deterministic hazard assessment and implementation of local site effects in the hazard estimates. The studies presented in papers 1-3 address these issues to take a step forward towards reliable seismic hazard assessment in Istanbul. To provide a framework for the studies, the already available information is summarized in sections 2.1 and 2.2. Sections 2.3-2.5 summarize the work presented in papers 1-3 and section 2.6 discusses the future challenges and remaining issues with respect to the seismic hazard in Istanbul.

In the last part of this chapter, focus changes to Sumatra where a devastating M=9.3 earthquake hit in December 2004. This event provided a unique opportunity for ground motion modelling in a different dimension than what was the case for Istanbul. At the same time, important questions were raised regarding the importance of ground shaking in the damage caused by this earthquake and the general issue of ground shaking behaviour of very large earthquakes. The December 26, 2004 earthquake is introduced in section 2.7 and the ground motion simulations for the event, as described in paper 4, are presented in section 2.8. Section 2.9 discusses the future seismic hazard for the region.

2.1 Tectonics and earthquake activity in the Marmara Sea region

The Marmara Sea region of northwestern Turkey is a seismically active region, which has experienced many large earthquakes in the past. The dominating tectonic feature in the region is the North Anatolian Fault (NAF, Figure 1), which is an approximately 1200 km long fault zone passing through northern Turkey, accommodating the westward movement of the Anatolian Block with respect to the Eurasian plate as a consequence of the African-Eurasian collision. The Marmara Sea was probably developed as a pull-apart basin along the NAF, causing an increased complexity with the fault zone splitting into two main branches (e.g. Sengör et al., 2005; Figure 2).

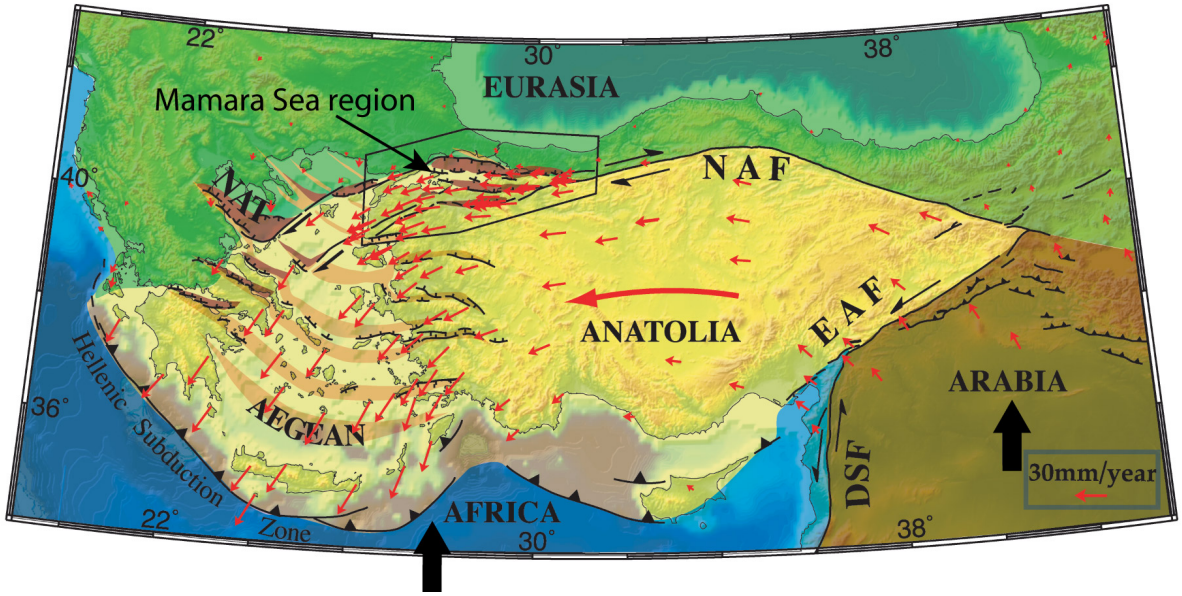

Figure 1. Plate tectonic setting for Turkey. NAF: North Anatolian Fault, EAF: East Anatolian Fault, DSF: Dead Sea Fault, NAT: North Aegean Trough. GPS vectors of McClusky et al. (2000) are shown as small red arrows. Modified from Armijo et al. (2005).

One branch (southern branch in Figure 2) continues south of the Marmara Sea whereas the other (northern branch in Figure 2) extends further north, under the sea. Some authors argue for a third branch striking through the eastern part of the central Marmara Sea (e.g. Okay et al., 2000, central branch in Figure 2) whereas others find no evidence for this (e.g. Imren et al., 2001). Based on GPS displacement vectors, Straub et al. (1997) conclude that the main part of the strain accumulation due to the

22±3 mm/yr plate motion takes place along the fault segment in the northern Marmara Sea, and this is therefore the most likely segment to break in a future large earthquake.

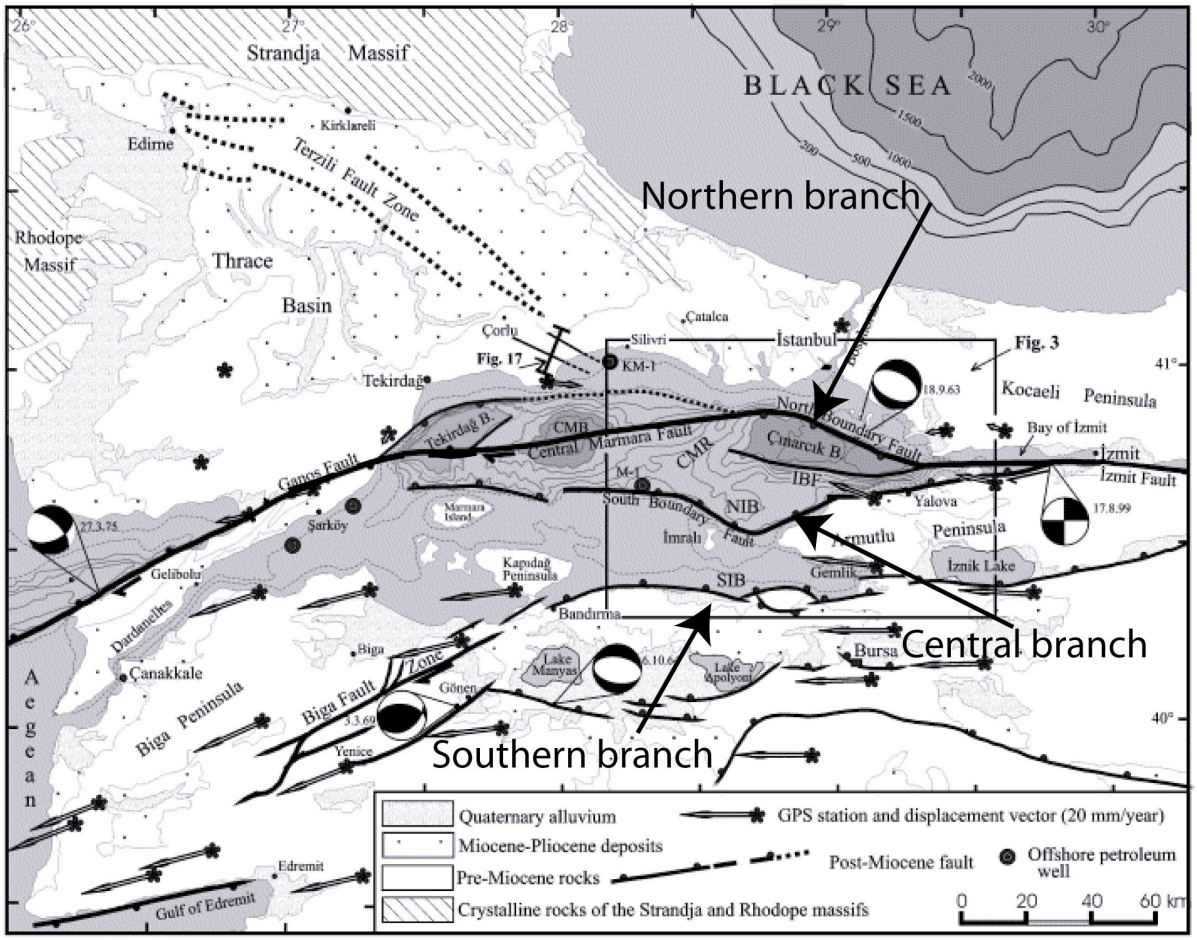

Figure 2. Tectonics of the Marmara Sea region as interpreted by Okay et al. (2000). The suggested three main branches of the NAF are pointed out. Modified from Okay et al. (2000).

The geometry of the Marmara Sea segment of the NAF has been much debated and a number of publications focus on this issue (e.g. Aksu et al., 2000; Imren et al., 2001; Le Pichon et al., 2001; Le Pichon et al., 2003; Yaltirak, 2002; Barka and Kadinsky-Cade, 1988; Wong et al., 1995; Ergün and Özel, 1995; Armijo et al., 2002; Armijo et al., 2005; Parke et al., 1999; Okay et al., 2000; Siyako et al., 2000). Several models have been proposed which can be subdivided into three main groups (Yaltirak, 2002). The groups represent rather different tectonic environments but are despite this all believed to tell parts of the truth representing different evolutionary stages of the system.

The first group of models describe the Marmara Sea as a pull-apart basin (Barka and Kadinsky-Cade, 1988; Wong et al., 1995; Ergün and Özel, 1995; Armijo et al., 2002; Armijo et al., 2005). The study of Barka and Kadinsky-Cade (1988) was the first modern study of the tectonics of the Marmara Sea based on seafloor topography and seismic data. They describe the northern Marmara Sea as a large pull-apart basin, which is sub-divided into smaller basins by NE-SW oriented strike-slip faults. Wong et al. (1995) and Ergün and Özel (1995) suggest a complicated tectonic structure where the NAF splits into en echelon structures bounded to the north and south by transtensional boundary faults. This separates the northern Marmara Sea into 5 rotating blocks of which 3 are pull-apart basins and 2 are push-up structures. Armijo et al. (2002, 2005) recognize significant fault step-overs sufficient to arrest rupture propagation of large earthquakes. These are due to pull-apart structures at different scales indicating a dominant transtensional tectonic regime in the Marmara Sea. As a consequence, a mixture of strike-slip and normal faulting is expected in this model.

The second class of models describe the NAF as splitting into several en echelon structures in the Marmara Sea (Parke et al., 1999; Siyako et al., 2000). Parke et al. (1999) describe the evolution of the Marmara Sea in terms of E-W trending normal faults. The model of Siyako et al. (2000) proposes three en echelon strike-slip faults crossing the Marmara Sea basins, in addition to shallow-dipping normal faults bounding the basins.

The third group of models define the NAF in the northern Marmara Sea as a through-going, continuous fault structure (e.g. Aksu et al., 2000; Okay et al., 2000; Imren et al., 2001; Le Pichon et al., 2001; Le Pichon et al., 2003; Yaltirak, 2002). Aksu et al. (2000) argue for a master fault below 5km depth, buried below a negative flower structure defining the principal deformation zone in the upper 5 km of the crust. Imren et al. (2001), followed up by Le Pichon et al. (2001, 2003), on the other hand, define a continuous strike-slip fault with two main parts (an 80 km long western part and a 65 km long eastern part). The eastern part boarders the Cinarcik basin and is affected by slight extension associated with the basin. Yaltirak (2002) agrees on the

description of a through-going master fault trending EW as an arc-shaped structure, but notes that this fault is buried in parts of the Marmara Sea. The model of Okay et al. (2000) suggests a single, through-going continuous fault consisting of four segments of varying orientation. These segments are (from east to west) the Izmit Fault, the North Boundary Fault (NBF), the Central Marmara Fault (CMF) and the Ganos Fault. This model differs from the single-fault models of Aksu et al. (2000), Imren et al. (2001) and Le Pichon et al. (2001, 2003) in suggesting a significant change in both orientation and fault mechanism between the CMF and the NBF segments.

The debate about the detailed tectonics of the Marmara Sea is still going on, but the discussion seems to converge towards an agreement on a continuous fault extending through the Marmara Sea (Le Pichon et al, 2003, Armijo et al., 2005). This represents a more mature stage of the basin evolution, in which the evolutionary stages could be explained as described for the first two groups.

Throughout the historical record, there are several examples of significant earthquakes in the Marmara Sea, some of which have caused great damage in Istanbul. The most recent ruptures of the northern strand of the NAF in the Marmara Sea are the 1509 M_s=7.2 and the 1766 M_s=7.1 and M_s=7.4 earthquakes. More recently, a smaller (M_s=6.4) earthquake ruptured the NBF segment in the Marmara Sea in 1963. East and west of the Marmara Sea, recent large ruptures have occurred with the 1912 M_s=7.3 Ganos earthquake to the west and the 1999 M_s=7.4 Izmit earthquake to the east (Ambraseys and Jackson, 2000). The general style of faulting along the NAF is right-lateral strike-slip faulting, but deviations from this occur in connection with changes in fault orientation. For example, earthquakes on the NBF such as the 1963 event usually have normal or oblique normal mechanisms (e.g. Sato et al., 2004).

Considering the seismic record of the last 500 years, the recurrence time of M=7+ earthquakes in the northern Marmara Sea seems to be 250-300 years (e.g. Ambraseys and Jackson, 2000). However, as noted by Ambraseys (2005), the predicted

recurrence times change depending on the length of observation interval, indicating that records are insufficient to determine exact recurrence times. Moreover, whereas there are repeated earthquakes in the Marmara Sea, the rupture segmentation does not seem to repeat. Instead, individual earthquakes rupture individual combinations of fault segments. An example is the area ruptured in the two earthquakes of 1999, most of which previously ruptured in a single event in 1719 (Mustafa Meghraoui, pers. comm., 2004). This illustrates that the five segments which ruptured during the Izmit earthquake (Barka et al., 2002) may, but do not necessarily have to, rupture jointly, a property which is expected to be valid for the entire NAF in the Marmara Sea region, posing additional challenges to seismic hazard assessment.

During the last century there has been a westward migration of large, destructive earthquakes along the NAF with the most recent events occurring in Izmit and Ducze in 1999 (e.g. Barka et al., 2002). Following these large events, there has been an increase in the coulomb stress along the Marmara Sea segment (Hubert-Ferrari et al., 2000), bringing this segment closer to rupture. Based on this observation combined with recurrence relationships based on the earthquake history in the Marmara Sea, the probability of a M=7+ earthquake in the Marmara Sea within the next 30 years has been calculated to be in the range of 35-70% (Parsons, 2004). This very high probability of a large earthquake poses new challenges in the assessment of seismic hazard, since the issue is no longer whether the earthquake is going to happen, but more a matter of how to mitigate the risk associated with the earthquake.

2.2 Previous estimates of seismic hazard in Istanbul

Since the 1999 Izmit and Duzce earthquakes, there has been an increased focus on the seismic hazard in Istanbul, and hazard assessments have been completed using both probabilistic methods (Atakan et al., 2002; Erdik et al, 2004) and deterministic scenario based ground motion modelling (Pulido et al., 2004). In the following, a summary of previously published material and a comparison of the results of different methodologies are given.

Atakan et al. (2002) applied probabilistic seismic hazard assessment (PSHA) following the 1999 earthquakes, comparing 12 models based on the combination of 4 attenuation models with 3 source models. For the source models, a standard poissonian model based on area sources was used in addition to two renewal models based on characteristic earthquake occurrence for two different combinations of area and fault sources. Each of the three source model were combined with four attenuation models; one based on European data (Ambraseys et al, 1996), two on western North American data (Boore et al., 1997 and Sadigh et al, 1997) and one based on a worldwide dataset (Campbell, 1997). A catalogue combined from data of the ISC, Ambraseys and Finkel (1995) and Eyidogan et al. (1991) was used as input in the modelling. The hazard results are given in terms of PGA values with a 10% probability of exceedence in 50 years for the northern Marmara Sea area around Istanbul. The computed hazard levels differ for the applied source and attenuation models, with the poissonian model predicting significantly lower ground motion values than the characteristic earthquake models. The highest PGA values are predicted in the eastern Marmara Sea close to the entrance of the Izmit Gulf. The largest ground motion levels are obtained for the Ambraseys et al. (1996) and Sadigh et al. (1997) attenuation relations. For these, maximum PGA values in the range of 30-35% g are predicted with PGAs of 25-30% g in southern Istanbul.

More recently, Erdik et al. (2004) performed a new seismic hazard analysis for the larger Marmara Sea region applying both deterministic and probabilistic methodologies. The deterministic analysis is based on a M=7.5 scenario earthquake in the Marmara Sea. A simple line source is combined with an attenuation relation to predict peak ground accelerations in the range 0.2-0.4g for southern Istanbul. The PSHA of Erdik et al. (2004) uses a combination of area earthquake sources and line sources based on the fault model of Le Pichon et al. (2001). For the attenuation, a logic-tree procedure is followed combining the relations of Boore et al. (1997), Sadigh et al. (1997) and Campbell et al. (1997) for a soft rock site. Two different recurrence models are applied, one assuming poissonian earthquake occurrence and the other using a renewal model. The predicted ground motion level is higher than

what is obtained by Atakan et al. (2002) with expected PGA values of 0.4-0.6g in southern Istanbul with a 10% probability of exceedence in 50 years. This difference is probably caused by Erdik et al. (2004) performing their calculations for soft rock site conditions whereas the Atakan et al. (2002) results are for bedrock conditions.

As discussed in section 2.1, several factors indicate that there is a high probability of a large earthquake occurring in the Marmara Sea within the lifetime of the present structures in Istanbul. This limits the gain from PSHA in that the main earthquake hazard is associated with a single, controlling seismic source, and a more realistic estimate of the hazard level would be obtained by predicting the ground motion caused by a large earthquake on this fault. This approach was followed by Pulido et al. (2004) who applied a hybrid method for simulating the bedrock ground motion caused by a M=7.5 scenario earthquake in the Marmara Sea. Their methodology combines deterministic calculations at low frequencies (0.1-1.0 Hz) with a semi-stochastic procedure at higher frequencies (1-10 Hz). This methodology has been applied in papers 2 and 4, where a more detailed description is given. As input for the modelling, a complex scenario earthquake source is defined in terms of location and dimensions of the rupturing fault and its asperities, source parameters such as rise time, rupture velocity and stress drop and properties of the surrounding crust in terms of velocity structure and attenuation characteristics. The input scenario of Pulido et al. (2004) is based on the fault segmentation model of Okay et al. (2000) assuming a combined rupture of the CMF and NBF segments. Three different hypocenter locations are tested to see the effect of rupture directivity. As output from the modelling, ground motion time histories are given at a number of simulation sites. Based on these, PGA and PGV distribution maps are created, which can be easily compared to the PHSA results. The largest ground motion levels in Istanbul are predicted for rupture initiation in the westernmost part of the CMF due to the effect of forward directivity towards Istanbul. In this case, PGA values up to 0.4g are predicted for southern Istanbul.

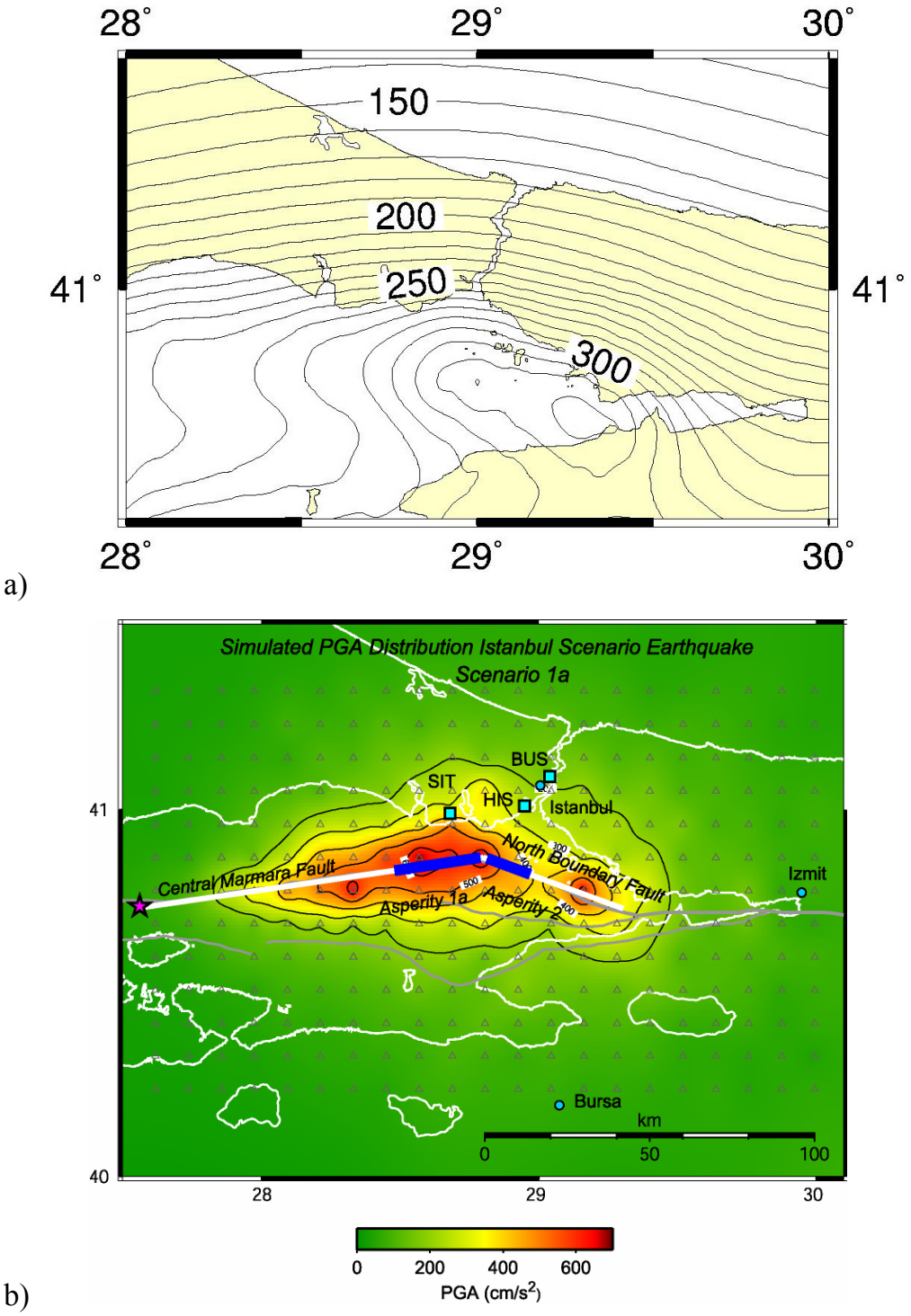

Figure 3. Comparison of PGA (in cm/s^2) distribution in Istanbul as predicted by a) Atakan et al. (2002) for their model 3 and the attenuation relation of Ambraseys et al. (1996) and b) Pulido et al. (2004) for their scenario 1a.

Figure 3 shows a comparison of the PGA values predicted by Atakan et al. (2002) using their most conservative scenario (using a renewal model and the attenuation relation of Ambraseys et al. (1996)) and the PGA values in the Istanbul region

predicted by Pulido et al. (2004) based on ground motion simulations for a M=7.5 scenario earthquake in the Marmara Sea. The probabilistic approach predicts significantly lower ground motion levels than what is obtained with the deterministic methodology. This indicates that the probabilistic methods may underestimate the actual hazard in the region. It should be emphasized here that the increased precision obtained by applying the deterministic approach only is valid because detailed information about the active faults and rupture dynamics in the region is available. Even in this case, the ground motion simulations are associated with significant uncertainties related to the input parameters for the modelling, an issue which is addressed in paper 2. Other advantages in applying deterministic methodologies is the much more detailed insight into the distribution of ground motion and the effect of source parameters. Outcome of the modelling is complete waveforms at the simulation sites. In this respect, we gain information about duration and frequency distribution of the ground shaking, which are important parameters for engineering applications.

2.3 A new attenuation relation for the Marmara Sea region

For the details of this study, the reader is referred to Paper 1

An important input parameter in seismic hazard assessments is the attenuation of seismic waves in the region of interest. For the Marmara Sea region, this issue has not previously been well resolved due to a lack of sufficient strong motion recordings in the region. As an alternative, attenuation relations from other regions of similar tectonics, usually California, have been applied in seismic hazard analyses. Recently, Özbey et al. (2004) performed a regression on a strong motion data set including the 1999 Izmit and Duzce earthquakes to obtain the first regional attenuation relationship for the Marmara Sea region. In comparison to their model, the empirical attenuation relations of western USA overestimate the ground motion in the region significantly.

In paper 1 we have followed an alternative approach for establishing an attenuation relation for the Marmara Sea region. Instead of basing a regression on limited strong motion data, we perform a regression based on the background seismicity providing a much more abundant dataset. The details of the regression are described in paper 1. We perform the regressions on events of magnitudes in the range $2.5<M_w<7.2$, recorded at distances between 10-200 km. These values set bounds on the validity of our final attenuation relation. We use a simple model in the regressions, assuming that the ground motion at a given site is a convolution of source, path and site effects. Following, the anelastic attenuation Q(f) and the geometrical spreading function g(r) have been fitted to the crustal propagation term through forward modelling. g(r) is modelled as a simple piece-wise linear function defined in two frequency bands separately. The best fit to the regressed data is obtained for the combination of g(r) as shown in Table 1 and Q(f) defined as:

$$Q=180(f/f_{ref})^{0.45}$$

where f is frequency, r is distance from the source and f_{ref} is the reference frequency described in paper 1.

Table 1. Geometrical spreading function for the Marmara Sea region as determined from regression on the background seismicity

Distance range	g(r), f < 1 Hz	g(r), f ≥ 1 Hz
r ≤ 30 km	$r^{-1.2}$	$r^{-1.0}$
30 < r ≤ 60 km	$r^{-0.7}$	$r^{-0.6}$
60 < r ≤ 100 km	$r^{-1.4}$	$r^{-0.9}$
r > 100 km	$r^{-0.1}$	$r^{-0.1}$

Predicted peak spectral accelerations (PSA) for a M_w=7.4 earthquake are compared to recordings of the 1999 Izmit earthquake and to PSA values predicted using attenuation relations of Özbey et al. (2004), Boore et al. (1997) and Atkinson and Silva (2000) for a firm-rock site at three frequencies in Figure 4.

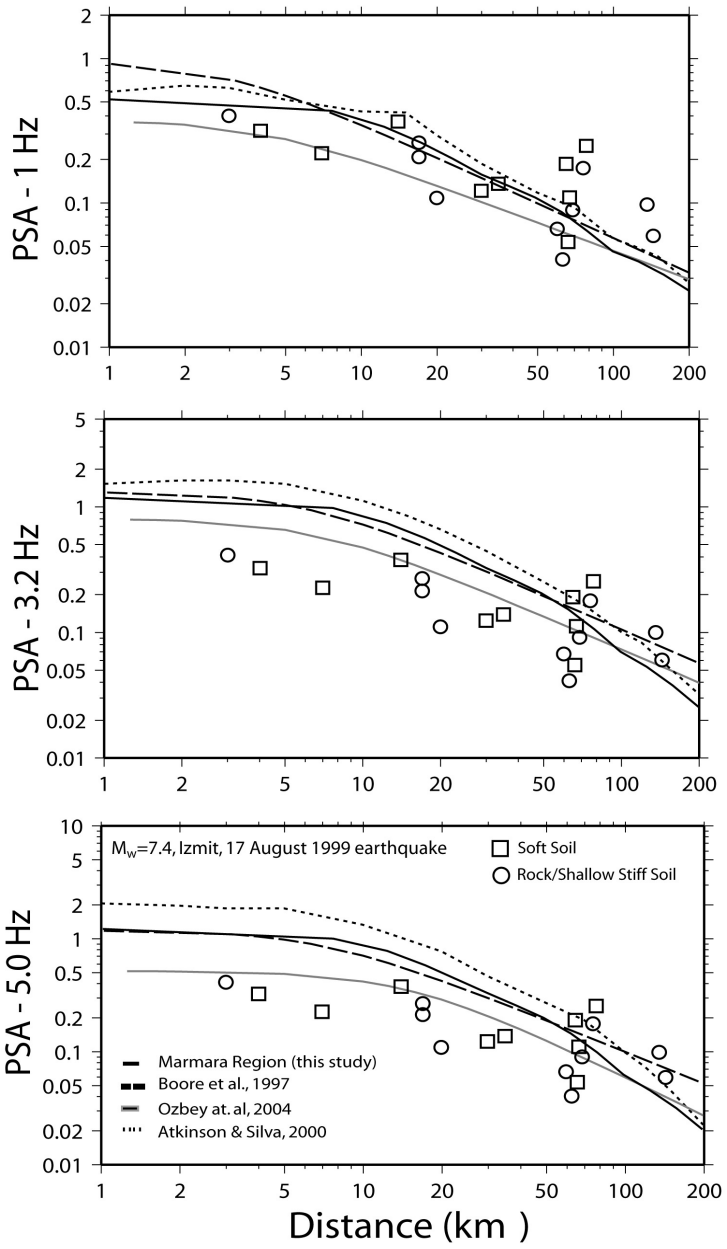

Figure 4. Comparison of different estimates of PSA (g) at frequencies of 1.0, 3.2 and 5.0 Hz in the Marmara Sea region as obtained by using the empirical relationships by Özbey et al., (2004), Boore et al., (1997) and Atkinson and Silva (2000); dark solid line indicates PSA computed based on the results of paper 1. Curves are computed for M_W = 7.4 and compared to the observed values of PGA (at soft, stiff and rock sites) during the 17 August 1999, M_W =7.4, Izmit earthquake.

The PSA values predicted by our attenuation model are in good agreement with the results of Boore et al. (1997) in the distance range 10-100 km. At distances shorter than 10 km we predict significantly lower PSA values, especially at 1 Hz. This is also the case for distances longer than 100 km where we predict lower PSAs for all frequencies. We generally predict lower PSA values than Atkinson and Silva (2000)

and higher values than Özbey et al. (2004) over the entire distance and frequency ranges. In comparison to previous PSHA results using e.g. the attenuation relationship of Boore et al. (1997) (such as Atakan et al., 2002; Erdik et al., 2004), the direct consequence of our attenuation relation will be a reduction of the seismic hazard predicted at distances less than 10 km and more than 100 km from the most active zones in the PSHA. For the city of Istanbul, assuming that the main earthquake threat arises from the NAF in the Marmara Sea, this will have little influence except in the northernmost part of Istanbul since most of the city is within 10-100 km distance from the fault, where the two relations show similar results.

To test the influence of the new attenuation relationship, it has been used as input in a set of ground motion simulations for a scenario earthquake of M=7.5 in the Marmara Sea. The result will be presented in section 2.4

2.4 Ground motion modelling for scenario earthquakes in the Marmara sea

For the details of this study, the reader is referred to Paper 2

As discussed in section 2.2, ground motion modelling provides a more sophisticated view on the seismic hazard in regions where the hazard arises from a single fault with high probability of breaking. The results of Pulido et al. (2004) give the hazard associated with one earthquake scenario and test the effects of varying rupture initiation point, asperity locations and attenuation relation. Other input parameters such as rise time, rupture velocity and stress drop are associated with significant uncertainties even in cases where the region is well studied, and the effect of varying these parameters on the simulated ground motion has previously been unresolved. To address this, we have made a detailed study on the effects of changing input source and attenuation parameters on the resulting simulated ground motion (paper 2).

For the modelling we followed the approach of Pulido et al. (2004), which is described in section 2.2. We performed the simulations for a reference scenario, which is an updated version of scenario 1a of Pulido et al. (2004), and changed source and attenuation parameters one by one in 15 test scenarios. The tested parameters are attenuation (in terms of frequency dependent Q), rise time, rupture velocity, rupture initiation point and stress drop (for details, see Tables 1 and 2 of paper 2). Our reference scenario is a relatively conservative approximation and thereby represents the upper bounds of the hazard in Istanbul. However, it should be noted that all calculations are at bedrock level, and the effects of local geology are not taken into account. The importance of local site effects in Istanbul and their implications for the seismic hazard are discussed separately in section 2.5 and in paper 3.

Figure 5 shows the distribution of PGA and PGV as modelled for the reference scenario. The predicted ground motion levels are slightly higher than what is obtained by Pulido et al. (2004), which is due to the asperities being located closer to the surface in our scenario.

For each of the test scenarios, the modelled ground motion is compared to the reference scenario in terms of peak ground motions, spectra and response spectra. We find that the most significant parameters in terms of ground shaking level are the rise time, rupture velocity, rupture initiation point and stress drop. The largest variability of ground motion is observed in adjacent regions to asperities as well as in the direction of rupture propagation. For PGV values, the variability decreases rapidly with increasing distance to the fault, whereas in the case of PGA values, the variability is distributed over a much wider region.

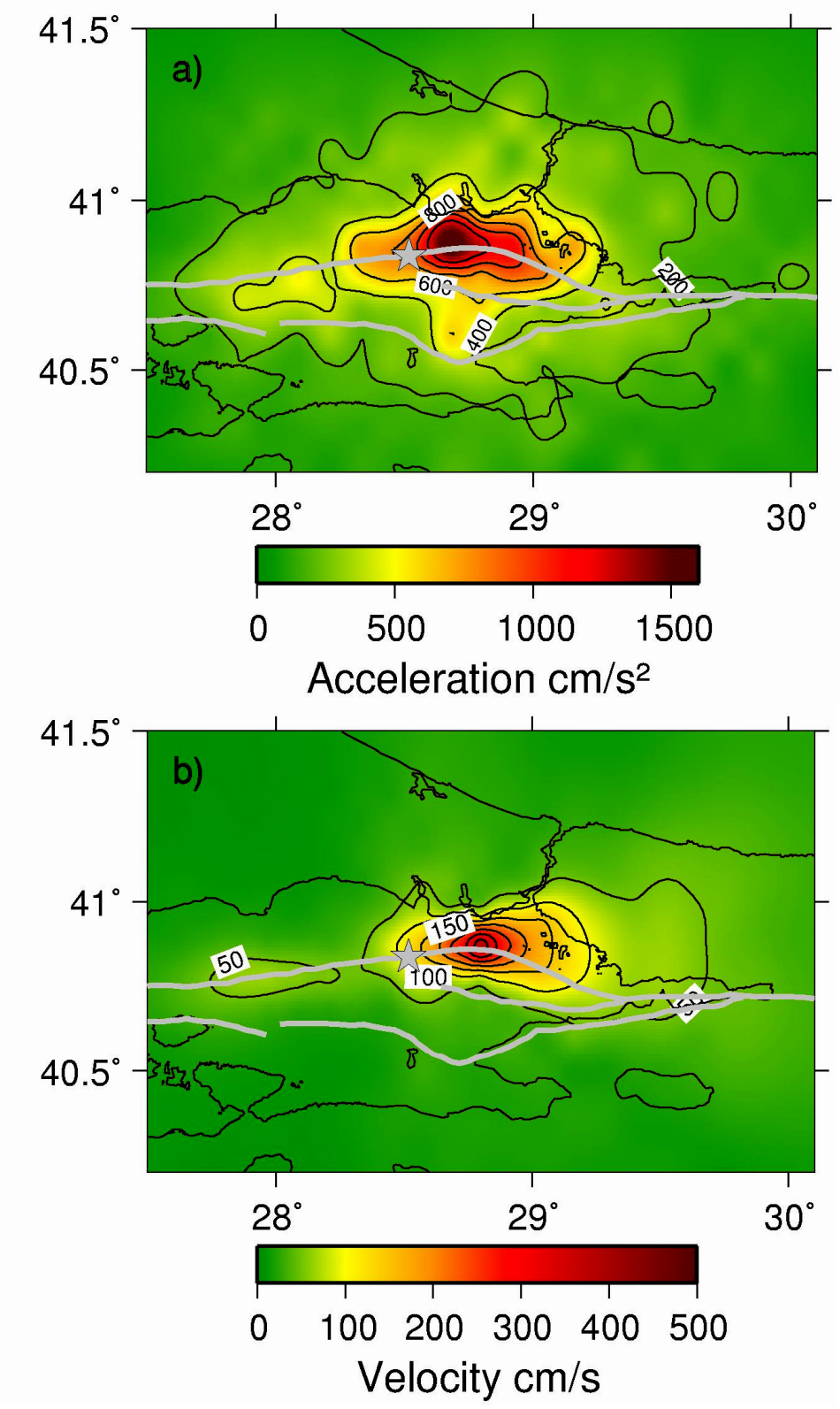

Figure 5: a) PGA and b) PGV distributions for the reference scenario of paper 2. Gray lines show the main faults of the region and the star indicates the epicentre.

Studying the spectral variation of the ground motion reveals that the different parameters have their main effect in different frequency bands and thereby have varying implications for engineering (see Figures 11-13 in paper 2). We observe that high-frequency ground motion is mainly controlled by the stress drop and Q, whereas rupture velocity and rise time have a strong effect on the low-frequency ground motion. For a number of selected sites in Istanbul, the bedrock response spectra consistently show peaks around 2 Hz as well as at longer periods (4 sec) (Figure 14 of paper 2). This implies a combined effect of large PGA values at high frequencies and large PGV values at longer periods, which could have a strong effect on the damage potential of ground motion for a wide range of buildings in Istanbul.

Figure 6 shows the distribution of standard deviations of the response spectra based on the 16 scenarios in three frequency bands. We observe that the variability of acceleration response spectra is strongly frequency dependent with a significant variation in the high-frequency part of the spectra. The velocity response spectra, on the other hand, are consistent, revealing the strength of ground motion modelling in estimating a realistic hazard for Istanbul and hence in risk mitigation efforts despite the large uncertainties involved.

In all previous ground motion models for Istanbul (Pulido et al., 2004 and the scenarios of paper 2), the input scenario earthquakes have been events rupturing the CMF and NBF segments in combination. However, one cannot exclude the possibility of a smaller earthquake (on the order of M=6.9-7.2 based on Somerville et al. (1999)) rupturing one of the segments individually, or an earthquake sequence similar to the ones observed in 1766 and 1999 rupturing the two segments with a time delay of up to several months. The latter case may have severe consequences since a second earthquake can destroy vulnerable structures, which have been damaged during the first event. Scenario based ground motion modelling for the individual rupture of the CMF and NBF segments will help resolving this issue. Such studies are already planned to be conducted in the future.

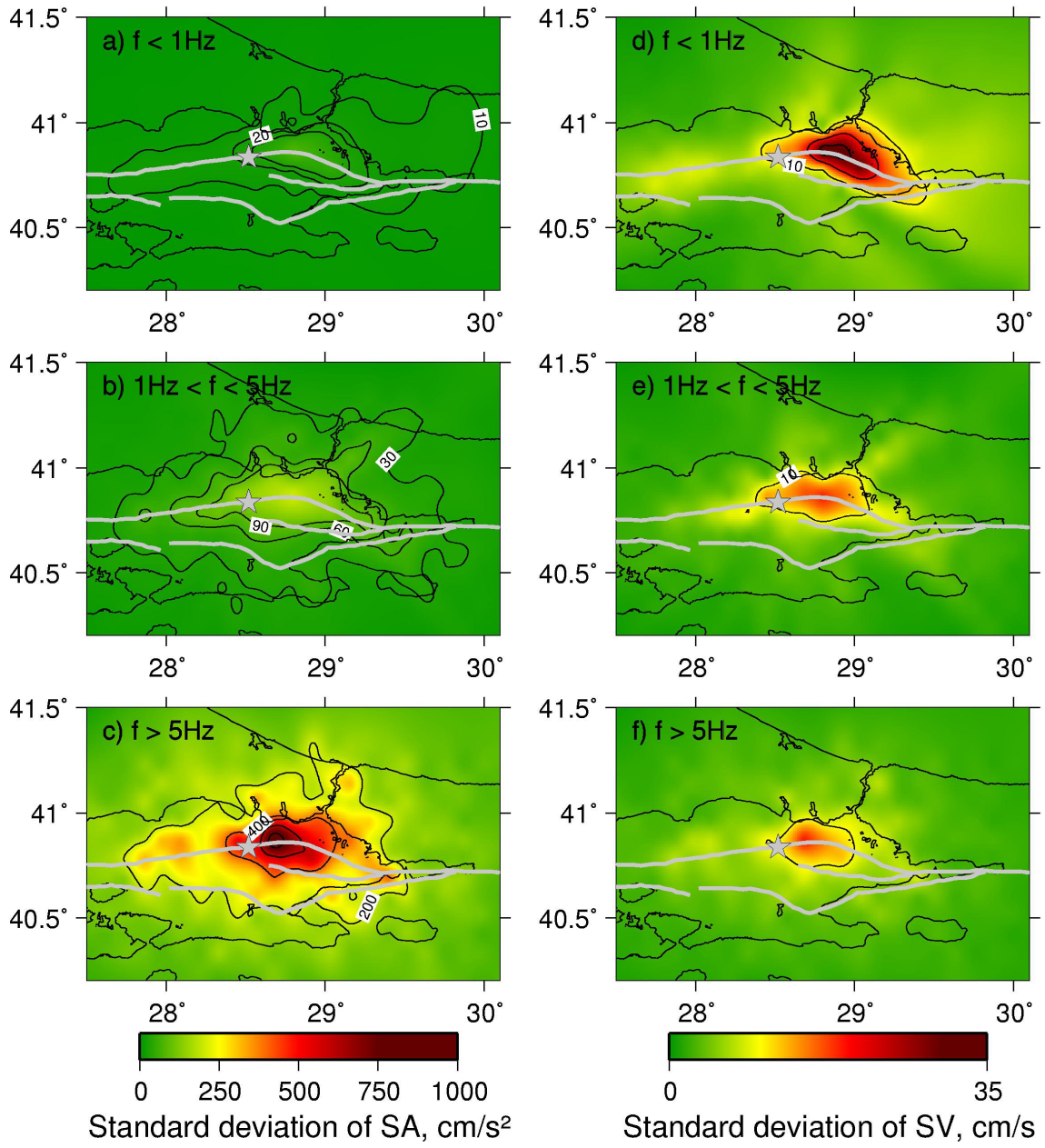

Figure 6. Distribution of standard deviation of response spectra for acceleration (a-c) and velocity (d-f). At each simulation point, the average value of the two horizontal spectral components is used. The average response spectral values are shown in three frequency bands: a,d) f<1Hz, b,e) 1<f<5Hz and c,f) f>5Hz.

One important aspect in terms of the likelihood of a large earthquake breaking the combined CMF and NBF fault segments is the significant fault bend (a large step-over) between the two segments and the ability of this bend to arrest fault rupture. This issue is addressed by Oglesby et al. (2005) through dynamic rupture modelling. They model the rupture propagation over three fault segments, two of which are strike-slip (analogue to the CMF and part of the Izmit Fault) and one normal

(analogue to the NBF). They conclude that ruptures initiating on the strike-slip segments are more likely to break the neighbouring segments than rupture initiating on the normal segment. The consequence of these results with respect to the seismic hazard in Istanbul is that the worst-case scenario with a combined rupture initiating on the western CMF segment and propagating also through the NBF is possible in terms of rupture dynamics, whereas a less conservative scenario with rupture initiation on the eastern NBF segment (and thereby less directivity towards Istanbul) is less likely to break also the CMF segment.

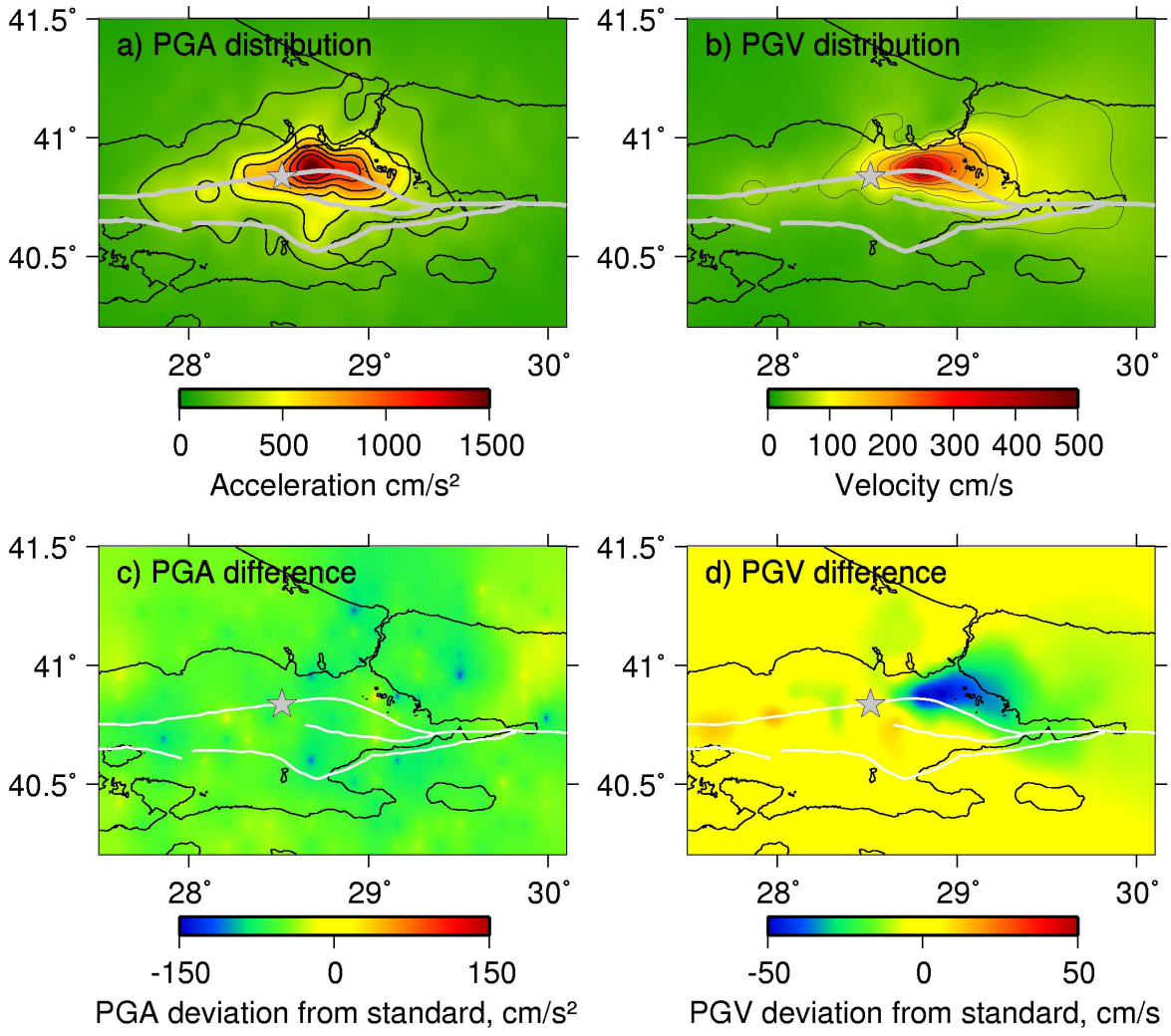

Figure 7. Simulation results for a scenario using the attenuation relation of paper 1. a) PGA distribution, b) PGV distribution, c) PGA difference to the reference scenario, d) PGV difference to the reference scenario. Major faults are shown as grey lines in a) and b) and as white lines in c) and d) and the rupture initiation point is shown as a star.

To test the effect of the new attenuation relation obtained in paper 1, an extra set of ground motion simulations have been performed using this relation ($Q=180 \cdot f^{0.45}$). The geometrical spreading function was not incorporated in the calculations. The resulting ground motion distribution and the difference from the standard scenario are shown in Figure 7. We observe that the results are very similar to what is obtained for scenario 1c ($Q=250 \cdot f^{0.5}$) of paper 2, as one would expect. Predicted PGA and PGV values are lower than for the reference scenario, decreasing the hazard level also onshore in Istanbul significantly.

2.5 Local site effects in Istanbul

For the details of this study, the reader is referred to Paper 3

Recently, there has been an increased attention towards the issue of local site effects in Istanbul. In this regard, possible effects of local geological variations have been studied in several microzonation studies (e.g. JICA, 2004; Eyidogan et al., 2000; Ansal et al., 2004). Birgören et al. (2004) found amplification levels up to a factor of 7 for some geological formations at 1 and 3 Hz frequencies, based on spectral ratios of records from a M=4.2 earthquake. In order to estimate the site effects present at all rapid response (RRS) station sites of the Istanbul Earthquake Early Warning and Rapid Response System (IEEWRRS, see section 2.6), a comprehensive microtremor survey was conducted by the Kandilli Observatory and Earthquake Research Institute (KOERI, Özel et al., 2005).

As mentioned above, and supported by the recent studies, the simulated ground motions need to take into account local site effects in order to provide more reliable hazard estimates. This has been the motivation for paper 3, which can be considered as a pilot study for the local site effects in the limited Ataköy area, with the aim of demonstrating the importance of the site effects and a possible implementation to hazard assessment.

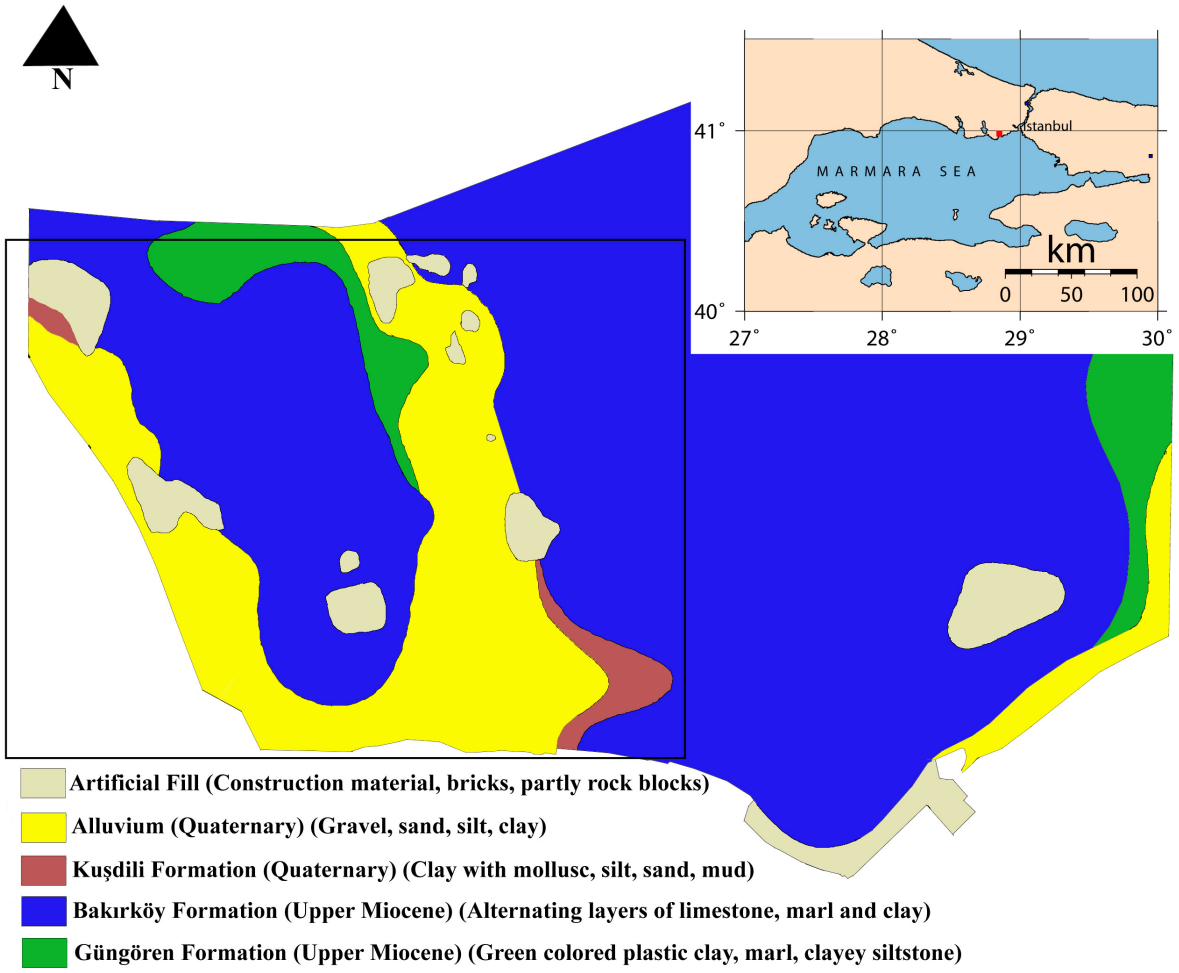

Figure 8. Geological map of the Ataköy and Bakirköy districts, western Istanbul. The location of Ataköy, as indicated by the black box, is marked by the red square in the index map. Colours represent different geological formations. The map is provided by Istanbul Technical University.

The Ataköy area is located in the southwestern part of Istanbul in an area dominated by geological formations composed of mainly limestone, marl and clay, and by alluvial deposits. In this respect, the region is expected to experience significant site amplifications and provides a good target area for our study. Figure 8 shows a geological map of the Ataköy area, which is dominated by the Bakirköy formation and the underlying Güngören formation, both of upper Miocene age. The Bakirköy formation is composed of alternating layers of limestone, marl and clay, whereas the Güngören formation consists of green coloured plastic clay, marl and clayey siltstone. In addition, the Quaternary Kusdili formation outcrops in limited areas. The Ataköy area is confined by two alluvial systems, which are the result of fluvial activity and consist of unconsolidated sediments composed of gravel, sand, silt and clay. We have

estimated the local site effects in Ataköy following three different approaches including 3D finite difference (FD) modelling, studying H/V spectral ratios of recorded microtremor data and 1D modelling of ambient noise.

For the 3D FD modelling, we applied a hybrid procedure in two steps (Oprsal and Zahradnik, 2002; Oprsal et al., 2002; Oprsal et al., 2005, see also Figure 3 of paper 3). In the first step we calculated the bedrock ground motion on an excitation box surrounding the site of interest using the methodology of Pulido et al. (2004) for a regional velocity structure. In the second step, the excitation ground motion is propagated through the local velocity structure to obtain surface ground motion expressed in terms of spectral amplification. The local velocity model is built from available geological, geotechnical and geomorphological data as described in detail in paper 3. The simulation results are shown in Figure 9, which gives a map view of the amplification factors in a number of frequency bands for the 3D FD modelling as well as for a pseudo 3D modelling based on a series of approximately 3 x 10^5 1D-structure-response computations for points regularly distributed on the free surface. The results show that significant site effects can be expected in the Ataköy area with amplifications up to a factor of 2 for the alluvial systems and lower amplifications for the firmer Bakirköy and Güngören formations. Amplification is present for the alluvial systems at all frequencies, increasing with increasing frequency, a tendency which is also present, but less pronounced for the surrounding formations.

In order to test the results of the 3D FD modelling, microtremor data were collected at a total of 30 sites, and studied in terms of H/V spectral ratios (Nakamura 1989, Nakamura 2000, Lermo & Chávez-García 1993). The recording sites are separated into two groups located on alluvium and on the Bakirköy formation, respectively. For the alluvial sites, a strong peak is observed around 1 Hz and a more diffuse peak is indicated around 3-6 Hz (see Figure 8 of paper 3). For the Bakirköy formation, there is again a clear peak around 1 Hz, whereas no peaks are observed for higher frequencies (see Figure 9 of paper 3). This indicates that the 3-6 Hz peak observed for the alluvium is an effect of the alluvial layer, whereas the 1 Hz peak is caused by

deeper lying formations. These results are, to some extent, in agreement with the 3D FD results, but some differences are observed. Most pronounced is the discrepancy in peak frequency for the deeper formations. This is probably due to inaccuracies in the velocity model and underlines the importance of good geotechnical data, an issue which should be addressed in the future.

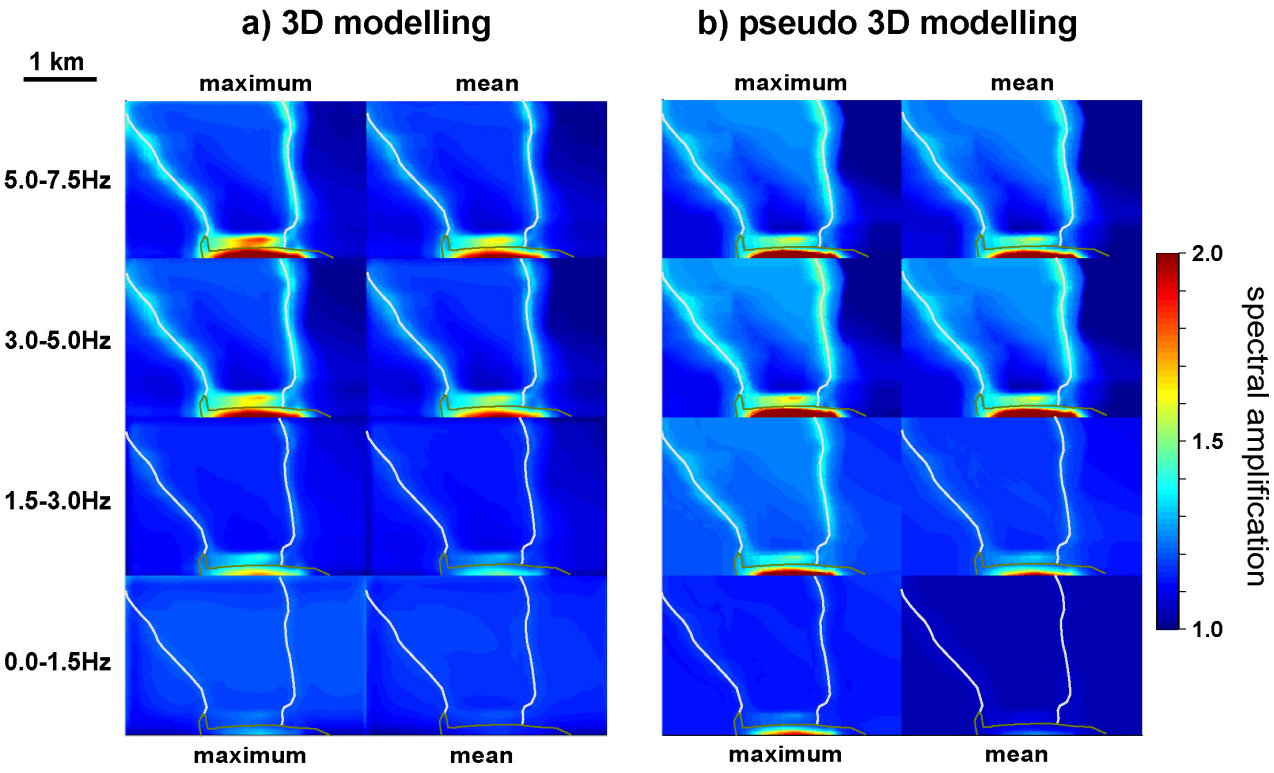

Figure 9. a) Spectral amplification (pseudo-acceleration response PSA, damping 5%) with respect to a bedrock site for 3D FD modelling for the area marked by the black box in Figure 8. The results are shown for a set of frequency bands; the left and right sides of the panel correspond to the maximum and mean PSA amplification. The amplified response of the southern part and of the two alluvial systems (marked by a white line) is apparent. b) Spectral amplification (pseudo-acceleration response PSA, damping 5%) with respect to a bedrock site for the pseudo 3D (1D) modelling. The results are shown for a set of frequency bands; the left and right sides of the panel correspond to the maximum and mean PSA amplification. The amplified response of the southern part and of the two alluvial systems is apparent.

The H/V spectral ratio results for recorded microtremors were compared to H/V spectral ratios calculated for simulated ambient noise. The noise simulations were performed as described by Bonnefoy-Claudet et al. (2004), simulating noise originated by human activity for sites with heterogeneous subsurface structure.

Ambient noise was simulated for three sites representative of an alluvial site, a site on the Bakirköy formation and a site on the Güngören formation, based on a simplification of the velocity model used for the 3D FD computations. The results show some significant differences compared to the results for the recorded microtremors, both in terms of peak frequencies and the relative magnitudes of the peaks (see Figure 11 of paper 3). The simulations show a diffuse peak at 1-3 Hz frequency and a stronger peak at higher frequencies for the alluvial site. The shift in frequency of the peaks is probably due to the reduced complexity in the modelling, and can possibly be accounted for by improving the 1D velocity models.

The study of local site effects in Ataköy shows us that this is an important issue that should be considered in future studies. Most significant amplifications are expected for the alluvial systems, but also the Bakirköy and Güngören formations are prone to site amplifications. Amplifications up to a factor of 2 can be expected, mainly in frequency bands around 1 Hz and 3-6 Hz. The geology in Ataköy is similar to what is observed in the neighbouring, densely populated Bakirköy and Zeytinburnu districts, and therefore similar site effects are expected here. Our results for Ataköy are in good agreement with the findings of Birgören et al. (2004) and Özel et al. (2005).

2.6 Future perspectives and challenges for hazard estimation

The assessment of seismic hazard in Istanbul is an ongoing process, and several questions remain to be answered in the future. One important line of work is towards the inclusion of local site effects in the ground motion modelling. This can be done either through the application of empirical Green's functions or by applying spectral site effects to simulated bedrock ground motion. Currently, studies following these lines of work are in progress.

Ground motion simulations in the region can be improved through more detailed studies of the fault behaviour in the Marmara Sea. Focus on characterization of the

fault parameters, fault segmentation, asperity locations, fault dynamics and the linkage between individual fault segments is of particular importance.

Another important issue is the coupling between seismic hazard and seismic risk. Once reliable estimates of the seismic hazard are obtained, these can be combined with vulnerability functions to estimate seismic risk. The increased awareness of the earthquake hazard in Istanbul has lead to several initiatives towards risk mitigation in Istanbul. One is the Earthquake Master Plan for Istanbul (IBB, 2003), which has resulted in the implementation of a number of mitigation plans such as a pilot microzonation study for the Zeytinburnu district, strengthening of the school and hospital buildings, etc. Another important initiative is the installation of the Istanbul Earthquake Early Warning and Rapid Response System (IEEWRRS) deployed by the KOERI (Erdik et al., 2003). The system aims to provide reliable information in case of a significant earthquake in the region. The Rapid Response System (RRS), which is part of the IEEWRRS, is composed of 100 strong motion stations and is designed to provide shake, damage and casualty maps immediately after an earthquake for rapid response purposes. In addition, there are ten broadband seismic stations installed mainly in the eastern part of the Marmara Sea region, which constitute the Early Warning System (EWS) part of the IEEWRRS. The main aim of the EWS is to provide rapid information about the earthquake source parameters and issue early warning to relevant authorities.

Dealing with a population of more than 12 million people in a city dominated by poor construction practices poses severe challenges to the risk mitigation. Here both social, cultural and economical aspects are important and priority must be set on various initiatives depending upon what is feasible within the given limitations.

In addition to being an important tool in the case of a large earthquake, the IEEWRRS can be used in the hazard and risk assessment efforts in several ways. Since the installation of the system, two earthquakes have occurred of sufficient size to be recorded by a large number of the stations (magnitudes 4.2 and 4.1, respectively). These events, in addition to future earthquakes, serve as excellent

Green's functions to be used in ground motion modelling. There are ongoing efforts towards implementing these events as Green's functions with the methodology of Pulido et al. (2004). Another use of the IEEWRRS in risk assessment, which is currently being addressed, is to use modelled ground motion as input to test the response of the system for a given scenario earthquake for information about the level of damage to be expected in a future earthquake. These results are important with regard to the ongoing efforts of risk mitigation in the metropolitan area in terms of strengthening the critical buildings such as hospitals and schools as well as planning activities for future settlements in Istanbul.

2.7 The December 26, 2004 Sumatra-Andaman earthquake

On December 26, 2004, one of the largest and most devastating earthquakes in history stroke offshore western Sumatra. This earthquake and the accompanying tsunami waves caused more than 200 000 casualties and left millions of people homeless in the countries surrounding the Indian Ocean. An important question posed after the earthquake was related to the strong ground motion distribution in the region and its consequences in places like Banda Aceh where severe destruction was observed. Although much of the damage was associated with the accompanying tsunami, it is still not clear how much of the destruction was due to strong ground shaking. More generally, the properties of ground motion due to such large earthquakes have not been studied in detail previously. The dimensions of the very large earthquakes pose methodological challenges to the ground motion simulation techniques, which motivated us to test if it was at all feasible to simulate the event using standard techniques. To address these issues, we have modelled the ground motion caused by the December 26, 2004 earthquake, using the methodology of Pulido et al. (2004) (paper 4).

The earthquake occurred along the Sumatra trench where the Indian-Australian plate is subducting under the Sunda microplate at a rate of 6-6.5 cm/yr. Seismotectonics of

the convergent plate margin along the Sumatra trench are dominated by thrust earthquakes along the subduction zone. The NNE oriented motion of the Indian-Australian plate gives rise to an oblique collision, which results in strain partitioning (McCaffrey et al., 2000; Simoes et al., 2004). The trench perpendicular (ca. NE-SW) component of the plate motion is accommodated by the pure thrust earthquakes that take place along the coupled plate interface between the subducting Indian-Australian and the overriding Sunda plates. The shallow angle of subduction along this interface allows considerable stress accumulation and it is therefore capable of generating large thrust earthquakes. Occurrence of mega-thrust earthquakes (M>9) however, was not observed until the December 26, 2004 earthquake. The trench parallel component of the plate motion is accommodated by large strike-slip earthquakes that occur along two parallel strands of faults, the Great Sumatran Fault that lies on land, parallel to the west coast of Sumatra, and its offshore equivalent the Mentawi Fault (Prawirodirdjo et al., 1997; McCaffrey et al., 2000; Bilham, 2005).

Prior to the December 26, 2004 earthquake, there have been several large (M>8) destructive and tsunamigenic thrust earthquakes in the history. The most significant of these are the 1797 (M=8.4), 1833 (M=9.0) and 1861 (M=8.5) earthquakes that all occurred south of the December 26, 2004 earthquake rupture (Bilham, 2005; Lay et al., 2005). There have also been a few significant earthquakes with slightly smaller magnitude along the Nicobar (M=7.9) and Andaman (M=7.7) islands regions in 1881 (Ortiz and Bilham, 2003) and 1941, respectively. Occurrences of these large earthquakes are typical both in size and frequency for the Java-Sumatra subduction zone. In comparison, the December 26, 2004 earthquake differed both in its enormous dimensions covering a total fault area of almost 1300 km along strike with variable width of 160 to 240 km, as well as in its slip characteristics.

The December 26, 2004 event started with a rupture at a latitude around 3°N along the Sunda trench at a depth of about 30 km. The rupture reached up to 20 m slip with fast velocities (ca 3 km/sec) for the first 420 km (Sumatra segment), then slowed down for the next 325 km (Nicobar segment) with an average rupture velocity of 2.5

km/sec and 5 m slip (Lay et al., 2005). The remaining Andaman segment, which extends northwards for about 570 km, had very slow slip with, on the average, less than 2 m displacements, distributed over a time segment from 600 up to 3500 seconds. This has produced seismic signals and excited free oscillations of the earth, which could be recorded with very long periods up to 20 min (Park et al., 2005; Stein and Okal, 2005). The first 600 seconds of the seismic signal consisted of the faster Sumatra segment rupture at the southern end of the fault, which transitionally changed into a slower slip along the Nicobar segment. During this transition the width of the fault also narrowed down from 240 km to 170 km between these two segments (Bilham, 2005; Lay et al., 2005).

A number of source inversions were made immediately after the December 26, 2004 earthquake was recorded on global seismic stations. Based on the teleseismic records and the inversion schemes used, different earthquake source-slip models have been obtained and presented. The main uncertainty with regard to the source concerns the slip distribution and the variation of rupture velocity along the entire fault length of 1300 km. The initial 420 km have been successfully modelled by both Ji (2005), Yamanaka (2005) and Yagi (2004) and the following general consensus reached by several authors (e.g. Bilham, 2005; Lay et al., 2005; Ammon et al., 2005; Stein and Okal, 2005), agrees on the rupture characteristics of the southernmost Sumatra segment with its fast slip. On the other hand, the transition from fast to slow slip along the Nicobar segment and the following extremely slow slip generated by the northernmost Andaman segment are poorly understood with respect to their contribution to the resulting tsunami. It is important to note here that the total energy released is tripled due to this slow slip component, from the initial estimates of M_w =9.0 to a value of M_w=9.3. Although the slip was very slow, the geodetic data (GPS) indicate permanent deformations in the order of several meters along the Andaman segment (Bilham, 2005).

2.8 Modelling of ground motion for the December 26, 2004 earthquake

For the details of this study, the reader is referred to Paper 4

The ground motion simulations for the December 26, 2004 Sumatra-Andaman earthquake follow the methodology of Pulido et al. (2004), which is described in section 2.2. Paper 4 gives a detailed presentation of this study. Only the southernmost Sumatra and Nicobar segments of the rupture have been included in the modelling since the slow slip on the Andaman segment is not expected to contribute significantly to the ground shaking. The scenario source model is based mainly on the source model of Yagi (2004), which has been modified to take into account results of later publications. In order to account for the large variability of slip along the rupture, two groups of asperities with high slip (asperities 1 and 2) and intermediate slip (asperities 3-5) are defined (see Figures 2 and 3 of paper 4).

The simulated PGV and PGA distributions at bedrock level are shown in Figure 10. It is clear that the strongest ground shaking occurs close to the rupturing fault plane and that the reverse mechanism of the earthquake has a strong effect on the directivity of the ground motion. PGV values reach up to 200 cm/s above the fault plane and are strongest in the region near high-slip asperity 1 (marked in Figure 10). This is probably a combined effect of the large moment release and large size of this asperity and the proximity to the rupture initiation point. On land in northern Sumatra, velocities reach values up to 100 cm/s at bedrock level. The PGA distribution differs significantly from the PGVs, and we observe significant PGAs (in the order of 0.5g) over the entire fault plane. The largest values of PGA are predicted in the area around asperity 1 reaching values of 1200 cm/s^2, but also high-slip asperity 2 and the intermediate-slip asperities have a significant effect on the ground accelerations. This has important implications for the Nicobar islands which have experienced significant accelerations. Largest bedrock accelerations on northern Sumatra are at the order of 0.4 g. Considering that the local site effects are significant for the area

around Banda Aceh, the modelled ground motion levels (60 cm/s PGV) may explain shaking intensities up to IX, as observed by eyewitnesses and a field survey. The duration of ground shaking was here modelled to be approximately 150 s (see Figure 8 of paper 4).

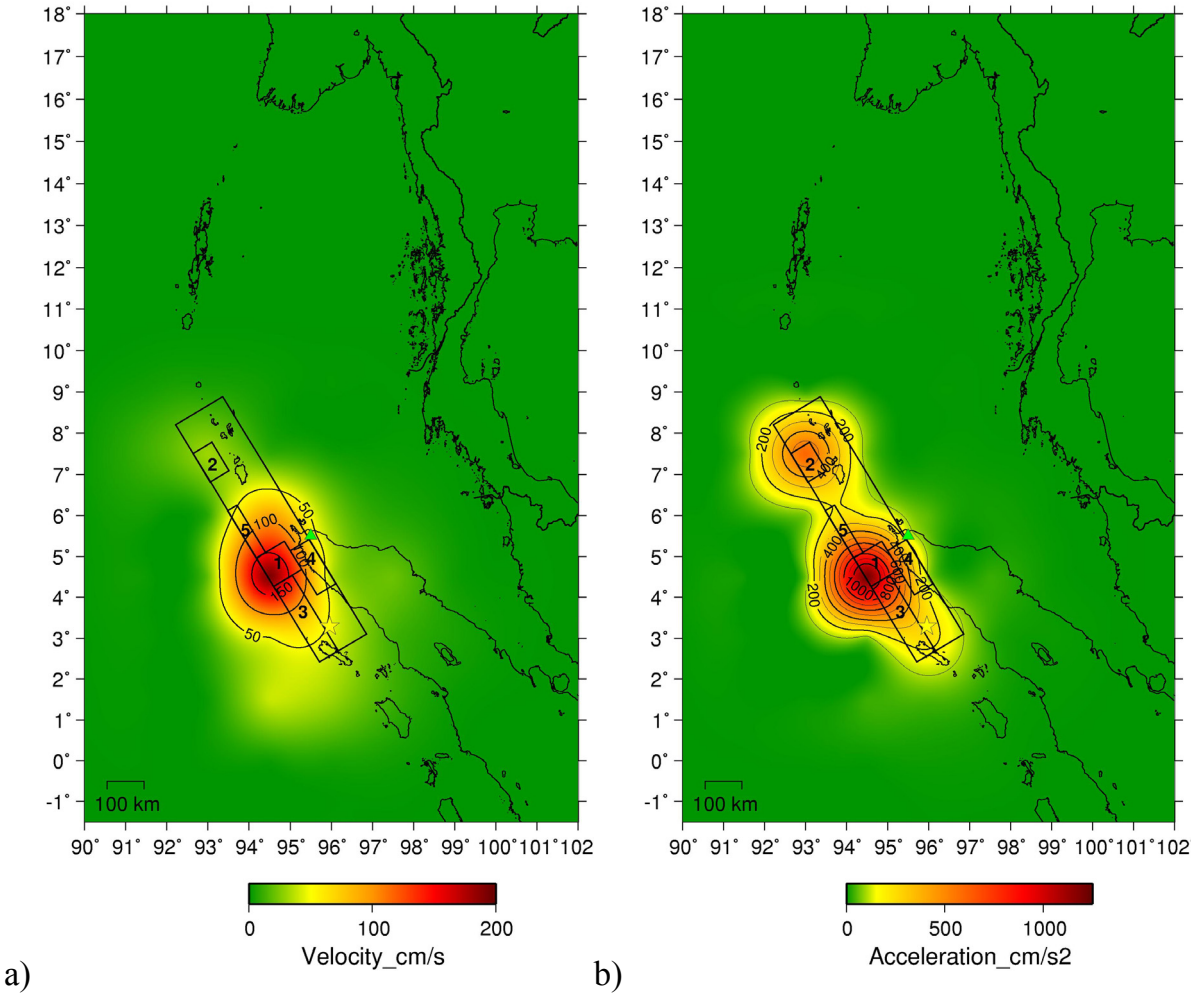

Figure 10. Simulated bedrock a) PGV and b) PGA distributions for the December 26, 2004 Sumatra-Andaman earthquake. The source model is shown as black boxes with numbers referring to the asperities as described in paper 4.

An important feature, which can be observed in Figure 10, is the attenuation of ground motion along the rupturing fault. It is clear from the distribution of ground shaking along the fault, that shaking originating from one end of the fault does not reach the opposite end. This underlines an important property of the ground shaking caused by very large earthquakes. Due to the large extent of the fault planes for such earthquakes, a single point even close to the fault will not be affected by the entire

amount of released energy due to attenuation occurring along the fault. Therefore there is an upper limit to the ground shaking level a given area can experience, which is more dependent on the amount of slip along the fault segments close to (i.e. within a few hundred kilometres from) the site of interest than on the total magnitude of the earthquake.

2.9 Future earthquake hazard in Sumatra

Following the December 26, 2004 earthquake, there has been an increased focus on the future hazard associated with earthquakes in the Sumatra trench and along the Great Sumatran Fault, both in terms of ground shaking and tsunamis.

Coulomb stress transfer modelling performed by McClosky et al. (2005), estimated positive stress changes along the southern part of the December rupture. These estimates were manifested by the earthquake of March 28, 2005 (M_w=8.7) that occurred along the southern part of the Sumatra trench close to the island of Nias. Similar calculations performed for optimally oriented strike-slip faults (Figure 11) have shown that the stresses have increased in the region near the Great Sumatran Fault, which may therefore have been brought closer to rupture. This fault has historically experienced earthquakes up to M=7.7 and is probably capable of generating events with magnitude up to 7.9 (Petersen et al., 2004). Such an earthquake, striking in the northern part of Sumatra, could have disastrous consequences in an area already severely affected by the strong ground shaking and tsunami wave of 2004. This issue should be addressed further in the future, for example through ground motion modelling similar to what is described above. Another important issue to be addressed is the probability of future tsunamigenic earthquakes along the Sumatra trench.

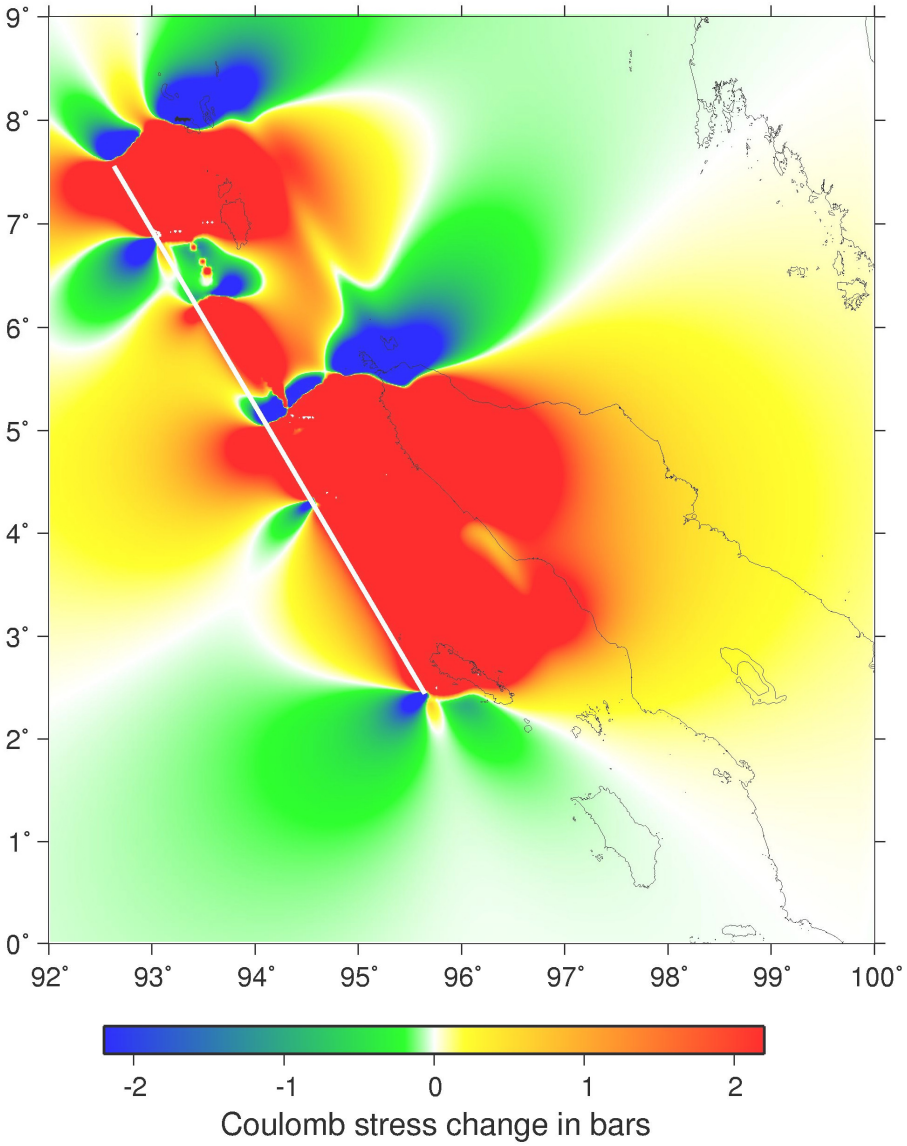

Figure 11. Result of coulomb stress modelling based on the December 26, 2004 Sumatra-Andaman earthquake. The fault plane of the model is shown as a white line.

3. Seismotectonics of selected areas in Norway

In comparison to the Marmara Sea and Sumatra regions discussed above, Norway is a seismically quiet place experiencing only moderate earthquakes occasionally. Due to this low seismic activity and the associated long seismic cycle, and to the offshore location of much of the Norwegian seismicity, there is a lack of knowledge regarding the coupling between the seismicity and active faults. The last three papers of this thesis address this issue, describing three regions of significant seismicity in Norway; the Jan Mayen, Rana and Skagerrak regions. Section 3.1, describing the tectonic evolution of the region and the overall seismicity, provides a framework for the papers. Despite the limited knowledge about active structures, seismic hazard assessments have been conducted and an overview of these studies is given in addition. Following, in sections 3.2-3.4, individual studies as presented in papers 5-7 are summarized.

3.1 Seismotectonic framework for Norway

A brief outline of the geological evolution of the Norwegian area is given in the following, based mainly on the description of Doré and Gage (1987): The Caledonian Orogeny, i.e. the collision of the Laurentia and Baltica continents, caused the closure of the Iapetus Ocean and creation of the Laurasian continent during Silurian/Early Devonian, approximately 400 Ma ago. Following the orogeny, fault-bounded molasse basins developed between the collided continents during Devonian as a consequence of sinistral translation of Laurentia relative to Baltica. Rifting took place in these basins throughout the Mesozoic until initial stages of sea floor spreading started during Early Cretaceous leading to the full break-up of the North Atlantic from Tertiary and onwards. The Carboniferous (280 Ma ago) Variscan collision of Godwanaland with Laurasia also affected the regions further north.

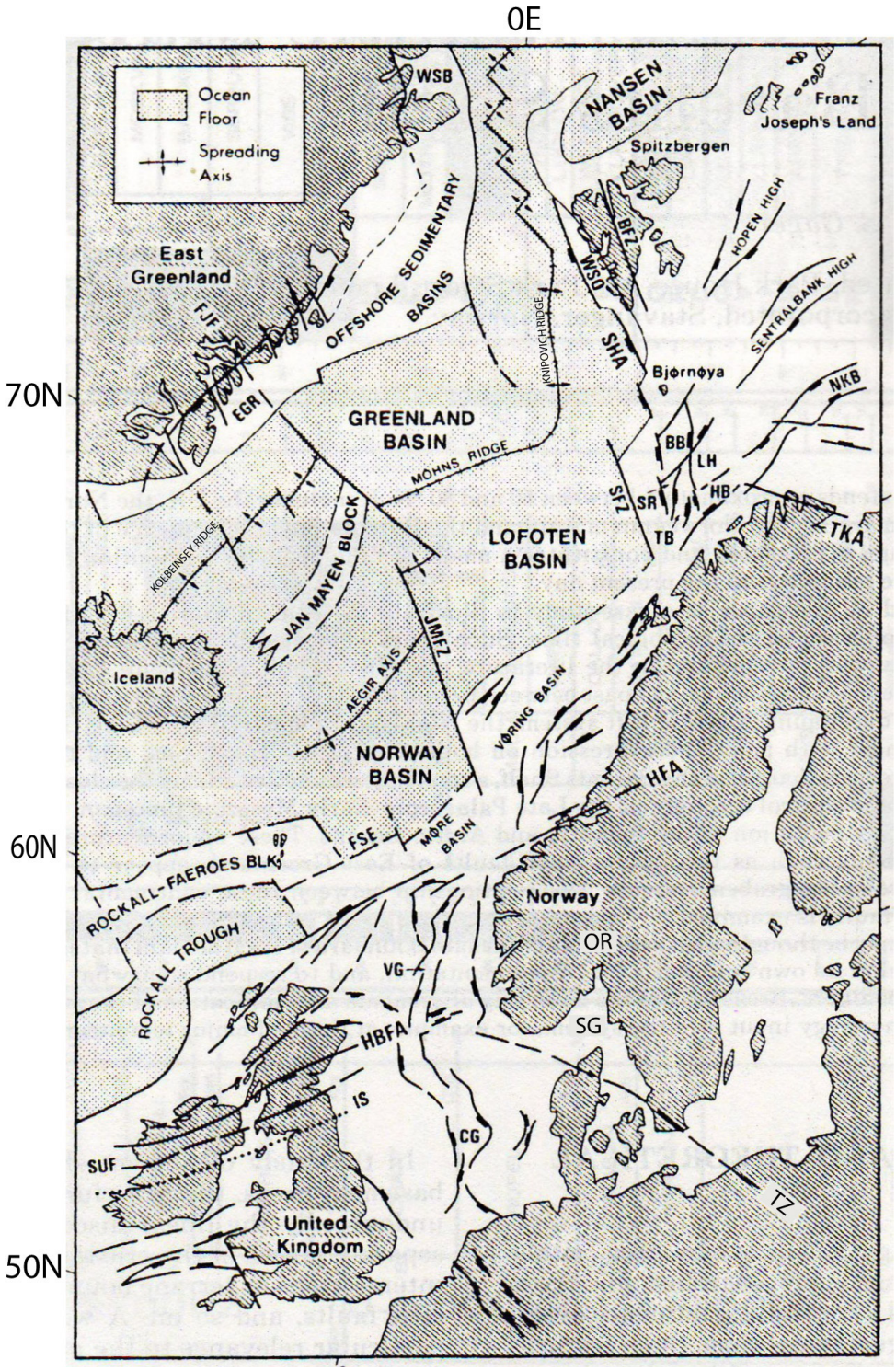

Figure 12. Main structural elements of the North Atlantic and surrounding areas. Abbreviations (only abbreviations for structures described in the text are included): CG: Central Graben, JMFZ: Jan Mayen Fracture Zone, OR: Oslo Rift, SG: Skagerrak Graben, TZ: Tornquist Zone, VG: Viking Graben. Modified from Doré and Gage (1987).

The Norwegian continental margin developed as a consequence of the Mesozoic rifting before break-up of the North Atlantic. The rift origin is reflected in the

present-day tectonics (Figure 12), which are dominated by numerous basin structures, the largest of which are the Vøring and Møre basins (Mosar et al., 2002). These basins subsided during Late Tertiary and Quarternary times (Bungum et al., 1991). In the North Sea, two important graben structures, the Viking and Central grabens, were created during the Mesozoic rift phases. The Tornquist Zone (TZ) is a major fault zone of Precambrian age, extending from the Black Sea to Skagerrak (Doré and Gage, 1987). It has been activated during several phases of the North Atlantic evolution. One example is during the Variscan collision, which resulted in left-lateral motion along the TZ. This lead to extension north of the zone, causing the creation of the Oslo Rift and its off shore continuation, the Skagerrak Graben (Doré and Gage, 1987).

The opening of the North Atlantic has occurred along varying rift axes leading to the creation of now extinct ridges and fracture zones such as the Aegir Axis and the eastern Jan Mayen Fracture Zone (JMFZ) in Figure 12 (e.g. Talwani and Eldholm, 1977). The present-day opening of the North Atlantic takes place along three main ridge segments. North of Iceland, spreading occurs along the Kolbeinsey Ridge until it reaches the JMFZ. The JMFZ is associated with a right-step and change of orientation of the spreading axis. North of the JMFZ, spreading takes place along the Mohns ridge to approximately 74°N where the orientation of the rift axis again changes and spreading continues along the Knipovich ridge.

The complex tectonic evolution described above has resulted in a present-day seismicity pattern dominated by significant activity associated with several elements. The seismicity of Norway, as recorded by the Norwegian National Seismic Network (NNSN), is given in Figure 13 for the time period 1985-2005. Most active is the plate boundary in the North Atlantic, but also some of the older structures are active. In this respect, extinct fracture zones such as the JMFZ and the Senja Fracture Zone, a large part of the continental margin and even parts of the stable continental interior show signs of significant activity.

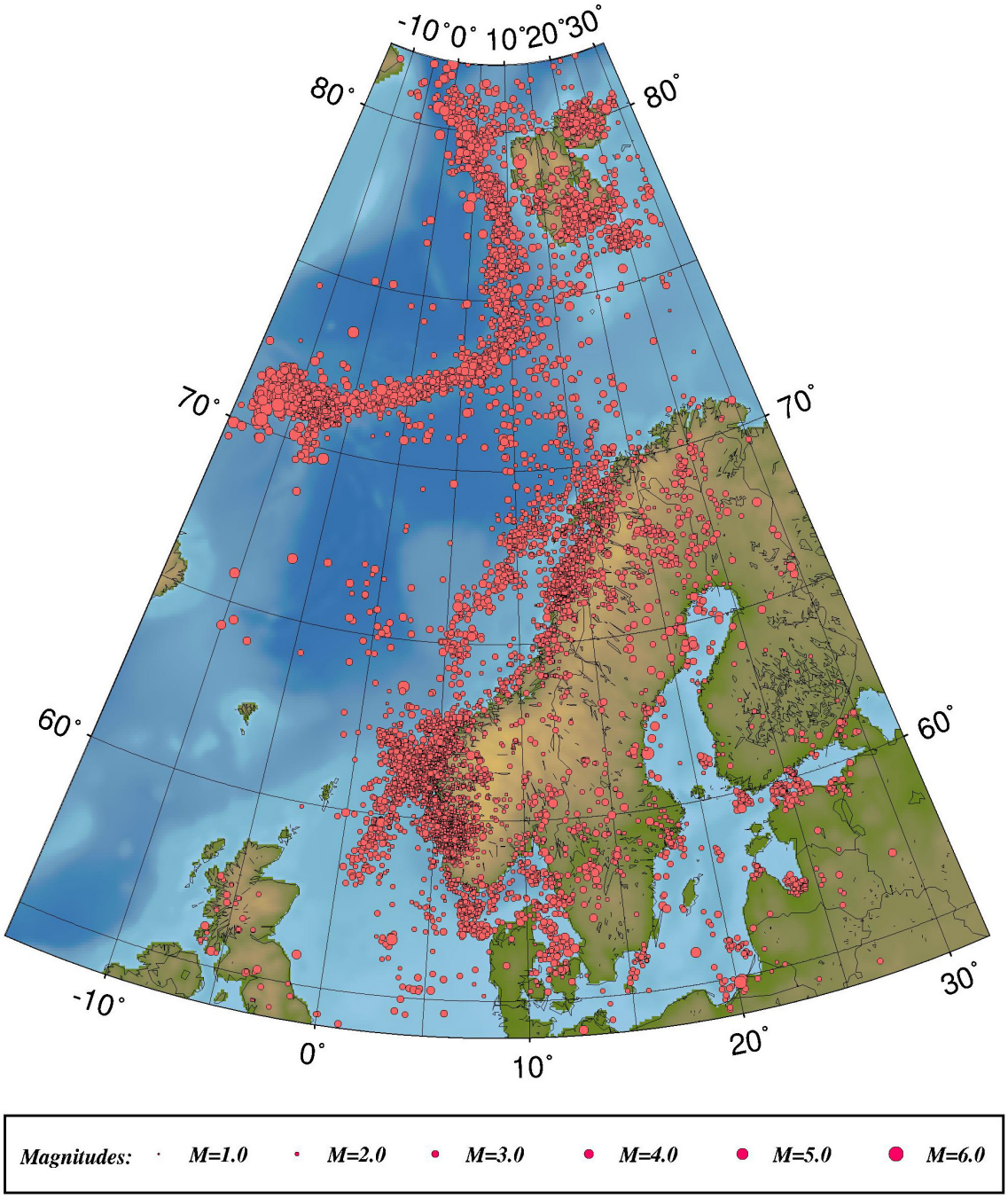

Figure 13.The seismicity of Norway and surrounding areas in the period 1985-2005 as recorded by the Norwegian National Seismic Network. Known and probable explosions have not been included in the map.

In the North Atlantic, there is a high concentration of earthquakes along the Mohns and Knipovich ridges. The increased activity around Jan Mayen is due to the short distance between the fracture zone and the seismic stations on the island leading to a lower detection threshold. In the JMFZ, M=6+ events occur regularly. This activity is discussed in paper 5. On the Norwegian mainland, the largest activity is associated

with the west coast. Offshore in the North Sea, a significant level of activity is associated with the Viking Graben, decreasing southwards in the Central Graben. Further north, activity is concentrated in two bands, one along the coast (an example from this region is discussed in paper 7) and the other associated with the offshore basins on the continental shelf. The Skagerrak Sea is another region of significant activity (paper 6). In the eastern part of Norway, moderate activity is present in the Oslo Graben.

The stress regime causing the earthquake activity has been described as originating from four main mechanisms (Fejerskov and Lindholm, 2000; Hicks et al., 2000a). Most important is the ridge push force due to spreading along the mid-Atlantic ridge. This gives rise to the general NW-SE oriented maximum horizontal compression. However, regional variations in the stress field are present, mainly due to crustal thinning on the continental margin and sediment loading in offshore basins and graben structures. Isostatic uplift due to deglaciation is believed to affect the stress field in parts of the Norwegian mainland. Based on 112 focal mechanism solutions in the Norwegian area, Hicks et al. (2000a) recognize a tendency of normal faulting onshore and strike-slip and reverse faulting offshore, which they explain through the regional effects on the stress field.

The largest earthquakes recorded on the Norwegian mainland are the 1819 M=5.8 Lurøy and the 1904 M=5.4 Oslofjord earthquakes. Both of these events occurred in regions of known activity. Especially the region around the Lurøy earthquake has been active with dominant swarm activity (Bungum et al., 1979; Atakan et al., 1994; Hicks et al., 2000a). This region is studied in more detail in paper 7.

Monitoring of earthquake activity in Norway is done by the Norwegian National Seismic Network (NNSN), which in March 2006 consists of 32 stations. The NNSN is run by the University of Bergen and includes also data from 3 array stations run by NORSAR as part of the International Monitoring System (IMS) of the Comprehensive nuclear-Test-Ban Treaty Organization (CTBTO). The studies described in papers 5-7 have made extensive use of data from the NNSN.

As already discussed, the assessment of seismic hazard for Norway is challenging due to the low seismicity leading to an incomplete dataset in terms of recurrence times and seismic zonation (Kijko and Sellevoll, 1990; Atakan et al., 1996; Lindholm and Bungum, 2000). This underlines the importance of seismotectonic studies to improve the seismic hazard assessment. Most studies on the Norwegian seismic hazard so far have been of regional extent with main focus on southern Norway and the North Sea (Ringdal et al., 1982; Bungum and Selnes, 1988; Kijko and Sellevoll, 1990; Singh et al., 1990; Atakan et al., 1996; Bungum et al., 2000). Singh et al. (1990) predicted peak ground accelerations of 30 cm/s^2 with a recurrence time of 100 years and 220 cm/s^2 with a recurrence time of 10000 years for southern Norway and the near offshore areas. The largest ground motion levels were predicted in the Oslo area and along the northern west coast. Kijko and Sellevoll (1990) focussed on the recurrence times for given magnitudes in western Norway, and estimated a M=5.0 earthquake every ca. 18 years and a M=5.5 every ca. 150 years. Atakan et al. (1996) also focus on western Norway and discuss the importance of geological information in hazard assessment in intraplate regions. They demonstrate how the inclusion of a fault structure only recognized from geological investigations increases the hazard level of the Etne area in western Norway significantly. Bungum et al. (2000) present a PSHA for all of Norway, the North Sea and the UK and present PGA values up to 1g with a return period of 475 years. The largest PGA values in Norway (PGA>0.6g) are predicted along the northern west coast, in the area of the 1918 Lurøy earthquake and in an area offshore mid Norway. In addition, two areas of elevated PGA are located near the British Isles.

The above-mentioned studies present interesting information about the general seismic hazard level in Norway and more detailed hazard distributions in well-studies areas, mainly in southern and western Norway. With the currently available information, there is little point in performing a new general hazard assessment for the whole Norwegian area, since the outcome is likely to be similar to what is obtained previously. What is presently lacking is more detailed assessments of the seismic hazard in other areas of significant seismic activity in Norway. In many of

these areas, basic information about the seismotectonics is missing and must be obtained before actual hazard assessment is attempted. Due to these limitations, it has not been attempted to assess the seismic hazard of Norway directly in this thesis. Instead, focus has been on studying the seismotectonics of selected regions to provide a better basis for future hazard studies.

3.2 Seismotectonics of Jan Mayen

For the details of this study, the reader is referred to Paper 5

Jan Mayen is a small volcanic island situated on the northern mid-Atlantic ridge north of Iceland. The high seismicity level and the occurrence of both tectonic and volcanic earthquakes make it an interesting location for studying the interplay of magmatic and tectonic processes.

The island is situated on the northern part of the Jan Mayen Ridge, which is of continental origin. The ridge is described as detached from Greenland as a consequence of a shift in the spreading axis from the Norway Basin, westwards to an intermediate axis located within the Iceland plateau around magnetic anomaly 7 (ca. 27 Ma ago). Approximately 13 Ma ago the spreading moved further westwards to the present location at the Kolbeinsey Ridge (e.g. Talwani and Eldholm, 1977; Grønlie et al., 1979). Following, there have been arguments against the suggested intermediate spreading axis (Vogt et al., 1980; Kodaira et al., 1998), however the continental origin of the Jan Mayen Ridge is well agreed upon.

Immediately north of Jan Mayen, the spreading axis is offset along the Jan Mayen Fracture Zone (JMFZ). The rate of plate motion along the JMFZ is 15-17 mm/yr (Kreemer et al., 2003; De Mets et al., 1990; De Mets et al., 1994). North of the fracture zone, on the western side of the Mohns Ridge, a small topographic ridge parallels the fracture zone, which develops into an approximately 60 km wide bank

opposite the island (Haase et al., 1996). This Jan Mayen Platform (JMP) was probably generated at a northward propagating spreading axis (Haase and Devey, 1994). A recent study of Svellingen (2004) suggests that the JMP is probably anomalously thick crust with the same petrophysical properties as the Mohns ridge and differing from the Jan Mayen island in its petrophysics.

Recent mapping of the bathymetry around Jan Mayen (Pedersen et al., in prep.) has provided much new information on the structural details of the JMFZ and the JMP. From the bathymetry (Figure 14 and paper 5) it is evident that the offset of the spreading axis along the JMFZ is accommodated by a NW-SE oriented left-lateral transform fault structure, named the Koksneset Fault. This is the only structure in the vicinity with sufficient size to generate M=6+ earthquakes. In the JMP a number of NE-SW oriented structures are mapped, which are expected to be normal faults accommodating the extension in the platform (Pedersen et al., in prep.; paper 5).

Volcanic activity on Jan Mayen is associated with the Beerenberg volcano at the northern part of the island. It has been suggested that this volcanism is due to hot spot activity (Wilson, 1973; Morgan, 1981; Schilling et al., 1983), but increasing evidence points towards an origin related to interaction between the continental ridge, the fracture zone and the spreading axis (Imsland, 1978; Haase et al., 1996; Svellingen and Pedersen, 2003). The volcano is highly active with an eruption frequency estimated to be 150±75 years by Sylvester (1975) and 100±133 years by Imsland (1986). The latest eruption was in January, 1985. Volcanic activity on the island is associated with volcanic tremors as studied by Havskov and Atakan (1991) for the 1985 eruption. They reported a large number of low-frequency events with waveforms differing significantly from tectonic events at the early stages of the eruption. In addition, tectonic events were triggered by the eruption (Havskov and Atakan, 1991).

Due to the location on a plate boundary, the seismicity of Jan Mayen and the surrounding regions is high with M=6+ earthquakes happening every 10-20 years (based on the ISC database). It has long been known that this seismicity was mainly

associated with the JMFZ and the spreading centres (e.g. Havskov and Atakan, 1991), but it has not been possible to associate earthquakes with specific fault structures. On April 14, 2004 a M_w=6.0 earthquake broke along the JMFZ. This event and its aftershocks have been studied in detail and compared to the recently mapped bathymetry of Pedersen et al. (in prep.) in paper 5, revealing new clues about the origin of the Jan Mayen earthquakes.

The April 14, 2004 main shock and aftershocks occurring within the first two months after the event have been located using data from the NNSN stations on Jan Mayen. Details about the location procedures are given in paper 5. Figure 14 shows the obtained locations together with the bathymetry of Pedersen et al. (in prep.). The main shock, shown with the fault plane solution of the Harvard CMT catalogue, is located at the western end of the eastern segment of the Koksneset fault. This fits well with the assumption that a large earthquake will occur along this structure with left-lateral strike-slip mechanism.

The aftershocks have been separated in two groups depending on the time of occurrence. Aftershocks within the first 12 hours after the main shock (blue dots in Figure 14) are used to outline the ruptured fault plane whereas later aftershocks (red dots in Figure 14) reflect the redistribution of stresses taking place after the main shock. The majority of the early aftershocks locate within a 10 km fault segment, which is believed to outline the fault rupture. The fault length of 10 km is in good agreement with what is predicted by Wells and Coppersmith (1994) for a M=6.0 strike-slip interplate event. The later aftershocks are more dispersed with two significant clusters of events in the JMP. These clusters are expected to be associated with activation of the normal fault structures in the JMP as a response to the main shock. The clusters locate at transfer zones oblique to the general NW-SE orientation and are expected to have oblique normal mechanisms. This is supported by coulomb stress modelling and is in agreement with the observed first-motion polarities of the events (see Figure 5 of paper 5).

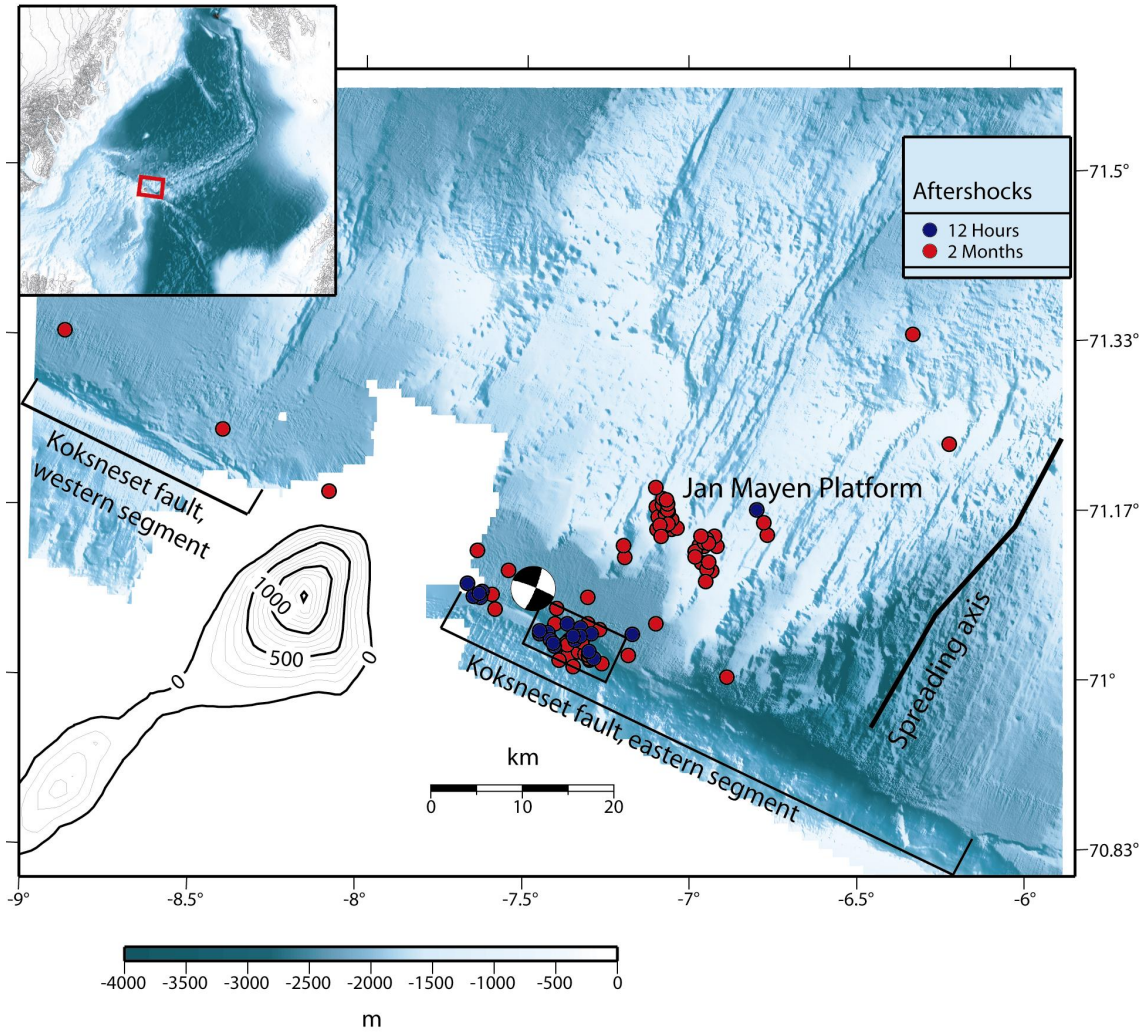

Figure 14. Earthquake locations plotted on the bathymetry. The locations of the Koksneset fault and the spreading axis (as located by Pedersen et al. [in prep.]) are indicated on the map. Contour lines are altitudes (in m) on Jan Mayen. The Jan Mayen Platform is located north of the Koksneset fault. The April 14, 2004 main shock is shown with the fault plane solution from the Harvard CMT catalogue. The blue dots are aftershocks occurring within 12 hours after the main shock; the red dots are later aftershocks occurring within 2 months after the main shock. The box outlines the extent of the ruptured fault plane from the aftershock distribution.

Prior to the 2004 event, the previous large earthquake in the Jan Mayen region was a M_b=5.7 event in 1988. Relocation of the largest aftershocks of the 1988 event using the same phases as for the 2004 event indicates that the two events occurred along the same segment of the Koksneset Fault (paper 5). Assuming full coupling, the expected recurrence interval for events of M=6 along a 10x10 km fault patch for a range of stress drops was calculated, assuming a spreading rate of 16 mm/yr and that slip

scales as the square root of the rupture area. The results indicate that a recurrence interval of 10-15 years, in agreement with what is observed in the area, would give full seismic coupling on a fault patch for earthquakes with stress drops of 0.5-1 MPa, which is in the range of stress drops found on ridge transform faults (Margaret Boettcher, personal communication, 2006; Boettcher and Jordan, 2004; Boettcher, 2005). This result is interesting because it indicates that the segment of the Koksneset fault rupturing in 1988 and 2004 is probably fully coupled, whereas neighbouring segments are probably slipping predominantly aseismically.

One issue that still remains to be resolved is the behaviour of the Koksneset Fault when it reaches the northern tip of Jan Mayen. During the summer of 2005, University of Bergen installed a temporary seismic station at the north tip of Jan Mayen. Data from this station will provide important clues of whether the Koksneset fault goes on land or remains offshore in this region. In addition, the data will help in constraining the earthquake locations, providing a more detailed view on the seismicity.

3.3 Seismotectonics of Skagerrak

For the details of this study, the reader is referred to Paper 6

The western Skagerrak Sea is an area of relatively high seismicity, as was illustrated in Figure 13 of section 3.1. Earthquake locations in the area have been associated with large uncertainties for two reasons. First, because of its offshore location neither the Danish nor the Norwegian seismic networks alone have sufficient coverage in the area, which limits the location accuracy. Second, the magnitudes of the events are small, implying that the available recordings are rather noisy. In 2003, NNSN installed the station SNART close to the southern coast of Norway, and thereby improved the registration capability of the Skagerrak earthquakes significantly. On

the Danish side, the nearest station to the Skagerrak is MUD located in northern Jutland (Figure 15).

Even though the geology of the Skagerrak area is well known, little has been done regarding the presence of active faults. Western Skagerrak is located in the Permian Norwegian-Danish Basin, bordered to the south by the Ringkøbing-Fyn-High and to the north by the Sorgenfri-Tornquist Zone (STZ) (e.g. Scheck-Wenderoth and Lamarche, 2005, see Figure 1 in paper 6). The STZ cuts through the northern part of the sea, marking a significant change in Moho thickness from the thick crust of the Fennoscandian Shield north of the zone to much thinner crust in the basin to the south (Lie and Andersson, 1998, see also Figure 2 of paper 6). South of the STZ, several N-S oriented fault systems, the Hummer, Krabbe, Kreps and Holmsland fault zones, cut the basin.

The Skagerrak seismicity has been the target of several studies (Gregersen, 1979; Gregersen et al., 1996a; Gregersen et al., 1996b). The results of these studies are a description of the seismicity as falling along an axis parallel to the Norwegian-Danish basin, NW from the shoulder of Jutland. No correlation is found to known fault structures. Gregersen (1979) locates the events close to the base of the crust at approximately 30-40 km depth.

In paper 6, seismotectonics of Skagerrak are studied in detail with the aim of correlating the present seismicity with known structures in the region. Here, earthquake locations are improved by combining available Norwegian and Danish data, and constraining event depths using data from the station SNART. Data from previous seismic profiles in the area have been reinterpreted and compared to the obtained earthquake locations.

Figure 15 shows the location of earthquakes in the Skagerrak for the time 1985-2005 after relocation. The most dominant feature is a N-S alignment of events between 6.5-7°E, south of the STZ to 57°N. Another dominant feature is the increased level of seismicity in the STZ. The N-S alignment of activity falls in the area between the

Kreps and the Holmsland fault zones, and does not seem to be associated with either of these. The activity in the STZ is expected to be associated with the bounding normal faults of the zone.

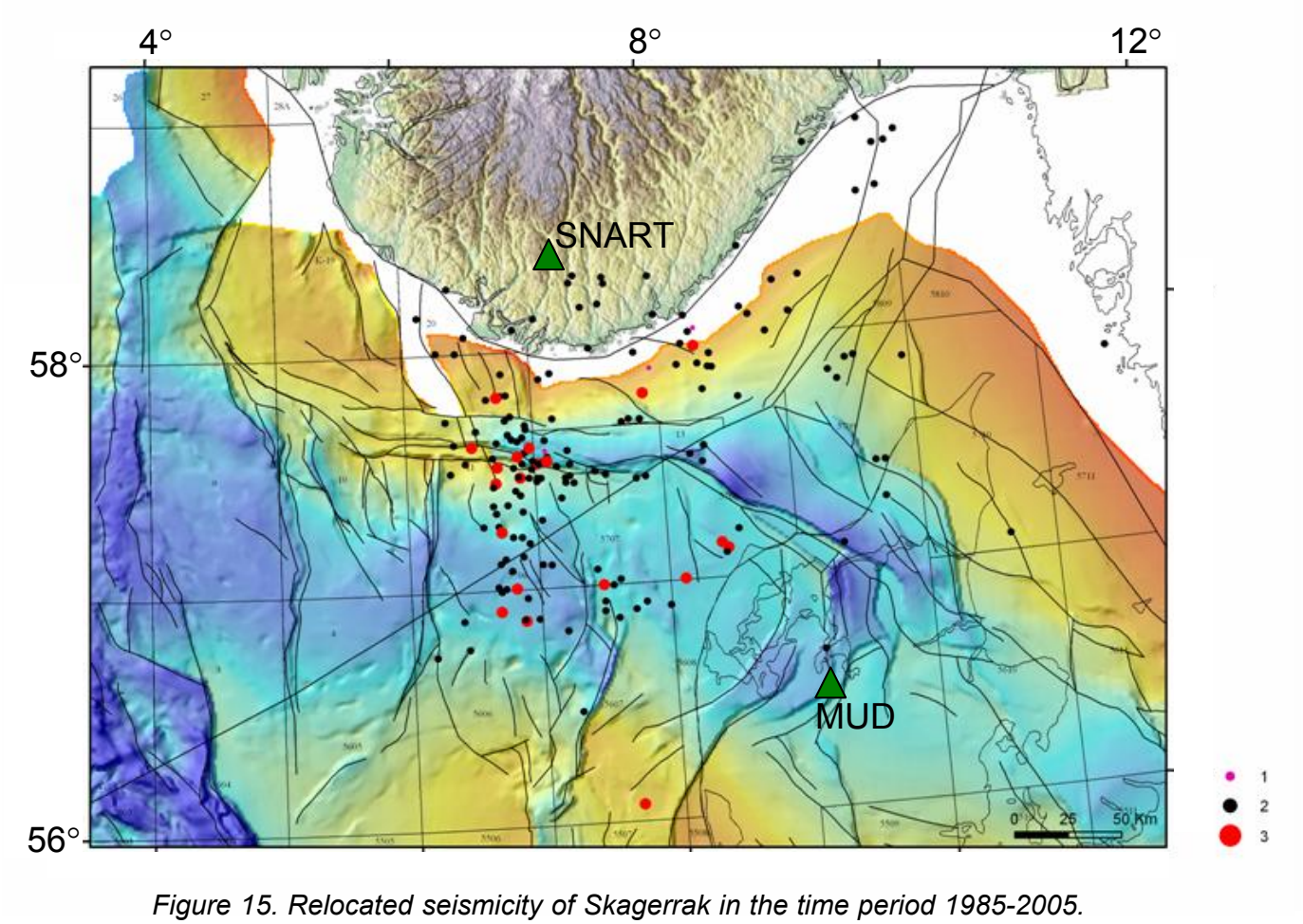

Figure 15. Relocated seismicity of Skagerrak in the time period 1985-2005. Lines show main tectonic features, for details see Figure 1 of paper 6. The locations of the MUD and SNART stations are indicated as green triangles. The events shown on the map are only the subset of the regional seismicity, which has been relocated in this study.

In order to study the activity falling between the Kreps and Holmsland fault zones, old seismic profiles crossing the area were reinterpreted. Figure 16 shows an example of such a profile. The Kreps and Holmsland fault zones are clearly visible extending to the Top Rotliegendes reflector (TR). In addition, a younger structure cuts between these fault zones in the area of the seismic activity. This structure is a previously unknown graben structure named the Langust fault zone. It extends through the Quaternary sediments, indicating recent activity. The events in the region are believed to be associated with this structure, breaking in normal, oblique normal or strike-slip events in agreement with the regional stress orientation (Gregersen, 1992;

Hicks, 1996; Hicks et al., 2000a; Reinecker et al., 2005) as well as the available focal mechanisms (Bungum et al., 1991; Gregersen and Arvidsson, 1992; Dehls et al., 2000). The relation of the Langust fault zone to crustal-scale structures is supported by gravity and magnetic anomaly data as discussed in paper 6 (see Figure 7 of paper 6).

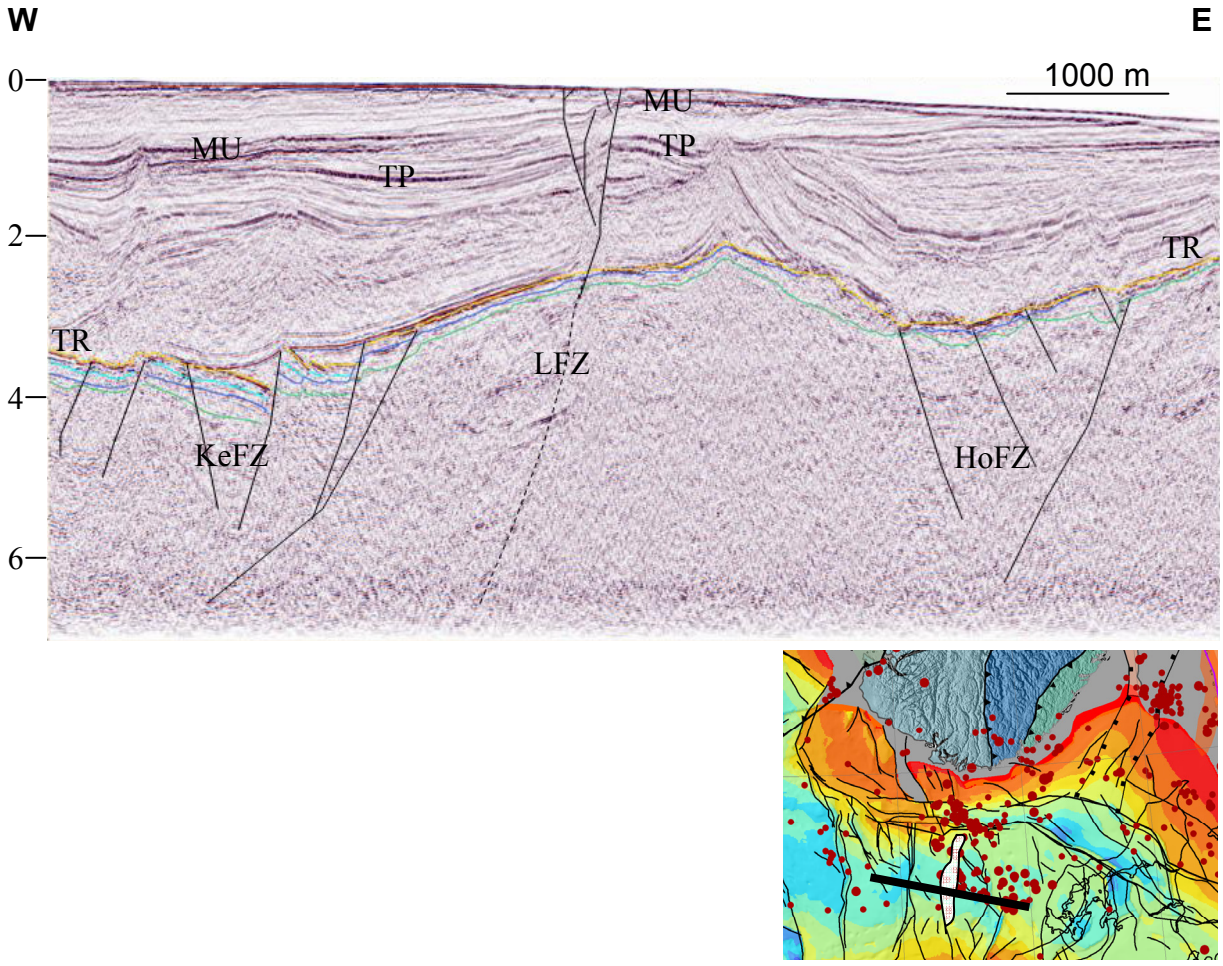

Figure 16. Seismic profile crossing the Langust fault zone. The new interpretation is plotted on top of the profile. The index map shows the location of the profile and the extent of the Langust fault zone. Letters indicate significant reflectors described in paper 6. The vertical scale is depth in kilometers. Abbreviations: TR: Top Rotliegendes; TP: Top Paleocene; MU: Base Miocene Unconformity; KeFZ: Kreps Fault Zone, LFZ: Langust fault zone, HoFZ: Holmsland Fault Zone.

3.4 Earthquakes in the Rana region, Nordland

For the details of this study, the reader is referred to Paper 7

The Rana region in northern mid-Norway is known to be one of the most seismically active areas in Norway and was the location of what is believed to be the largest historical earthquake in NW Europe, the 1819 Lurøy earthquake (M_S=5.8-6.2; Muir-Wood, 1989). The continuous high level of seismicity, which was evident after the installation of the NNSN station STOK in 2003, motivated a more detailed study of the activity, including the installation of two temporary seismic stations during the summer of 2005.

The seismotectonics of the region were studied by Hicks et al. (2000b) based on 18 months of data from a temporary local network. They concluded that the present-day activity is not associated with the neotectonic Bosmåen fault running parallel with the northern shore of the Rana Fjord. They located the events in five groups with NNW-ESE orientation at shallow depths ranging from 2-12 km. Nine focal mechanisms were calculated showing mainly normal and oblique-normal faulting, indicating a coast-normal orientation of the tensional stress component. This change in stress orientation in comparison to the surrounding regions is explained by local stress sources, most likely due to post-glacial uplift, which is at a maximum in the coastal regions. In addition, crustal inhomogeneities are mentioned as a likely origin. Swarm activity has been documented north of the Rana area in the Meløy swarm (Bungum et al., 1979) and the Steigen swarm (Atakan et al., 1994). These swarms show similar characteristics to the Rana earthquakes in terms of geologic and tectonic setting, which is reflected in similar shallow event depths, focal mechanisms and inferred stress orientation (Hicks et al., 2000b).

During the summer of 2005, two temporary seismic stations were installed in the area close to the NNSN station STOK with the aim of recording more of the small earthquakes in the region. Figure 17 shows the locations of these stations together

with all earthquakes in the region recorded by the NNSN during 2005. It should be noted that the detection threshold varies depending on the number of available stations through the year. The locations in Figure 17 are obtained using joint hypocenter determination (JHD) with all available recordings within 200 km distance. Due to very small magnitudes, some of the events are located based on data from only one station, and further investigations are necessary to obtain a complete and reliable picture of the seismicity. In general, the locations in Figure 17 confirm the observations of Hicks et al. (2000b) that the seismicity occurs in clusters, which do not seem to be associated with the Båsmoen fault located east of the most active area. Future investigations will reveal more details about the extents and orientations of the clusters.

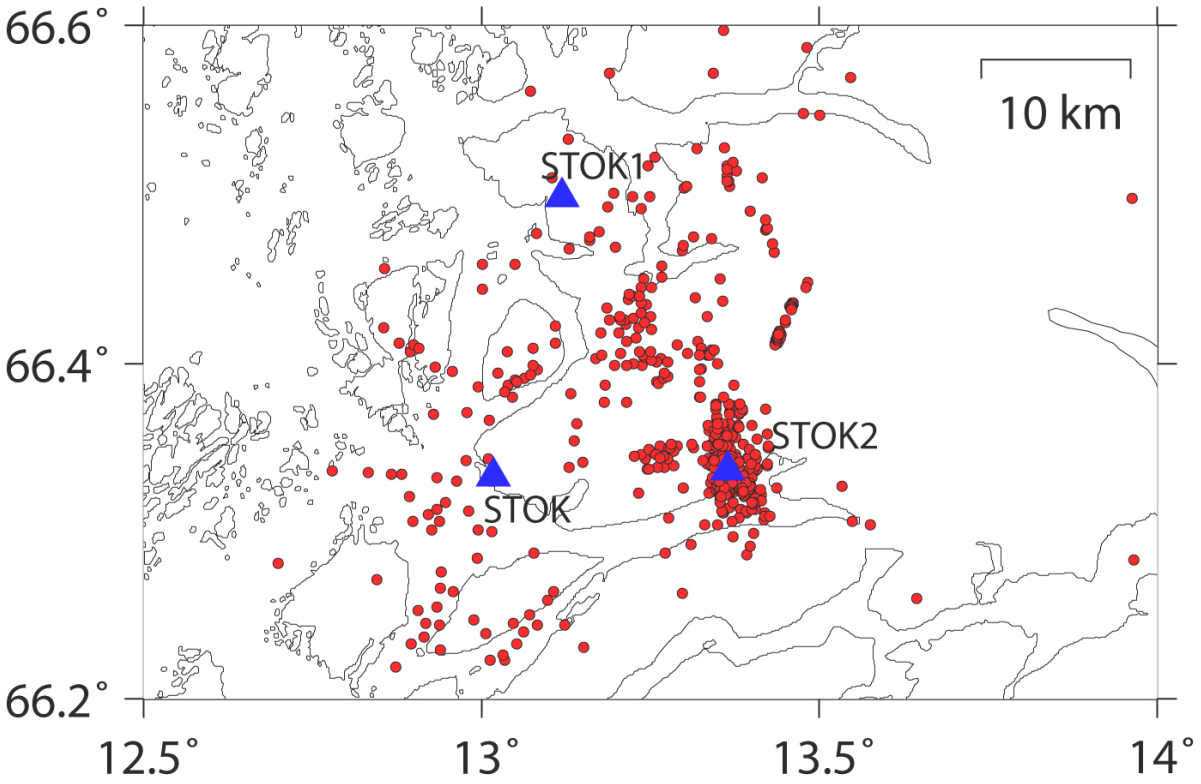

Figure 17. Location of earthquakes recorded by the NNSN in the Rana region during 2005. Locations of the stations STOK, STOK1 and STOK2 are shown as triangles.

In addition to providing important clues about the seismicity and seismotectonics in the region, the earthquake data provide excellent ground truth for testing event detection based on waveform correlation, which is the main topic of paper 7.

Event detection based on waveform correlation makes use of the fact that earthquakes with similar source mechanisms occurring close to each other will have very similar waveforms at a given seismic station. This has often been exploited in constraining event locations (e.g. Geller and Mueller, 1980; Waldhauser and Ellsworth, 2000; Menke, 2001) and for source classification (e.g. Israelsson, 1990; Harris, 1991; Riviére-Barbier and Grant, 1993; Schulte-Theis and Joswig, 1993). However, the use of waveform correlation for event detection is a relatively new field of study. This is due to the sensitivity of such detectors being constrained to a very small region around the master event and to the large amount of earthquakes occurring due to unknown sources. In recent studies, Gibbons and Ringdal (2004), Stevens et al., 2004 and Gibbons and Ringdal (2006) have applied an event detector based on waveform cross-correlation for array data to both mining explosions and earthquakes. Results of these studies are promising, showing extremely low levels of false triggers and a high stability for detection of controlled-source events. These methodologies can potentially provide a strong tool in the detection of e.g. mining explosions and swarm earthquake activity, but cannot replace simple STA/LTA based detection due to the large number of seismic events for which a master event cannot be obtained.

The event detector applied in paper 7 is the one described by Gibbons and Ringdal (2006). This is an array based correlation detector making use of the array geometry by beamforming the correlation traces at the individual stations, thereby increasing the sensitivity of the detector. A chosen master event is correlated against the various stations in the array and correlation traces are stacked with a time delay determined based on the master event.

During 2005, five events were recorded by more than one of the Scandinavian IMS array stations in the Rana region. The recordings of these events from the NORSAR array at a distance of ca. 600 km were compared through waveform cross-correlation, revealing three events with a high degree of similarity (Table 2, paper 7). The largest of these events was used as master event in a waveform correlation detector, which was run over continuous data from the NORSAR array for all of 2005. The detector

found 32 events of which one is believed to be a false trigger. The remaining 31 events were (except for one event) confirmed by performing similar cross-correlations at the other IMS arrays (Table 4, paper 7) and all events were recorded by the local network, confirming that these events had indeed occurred in the region.

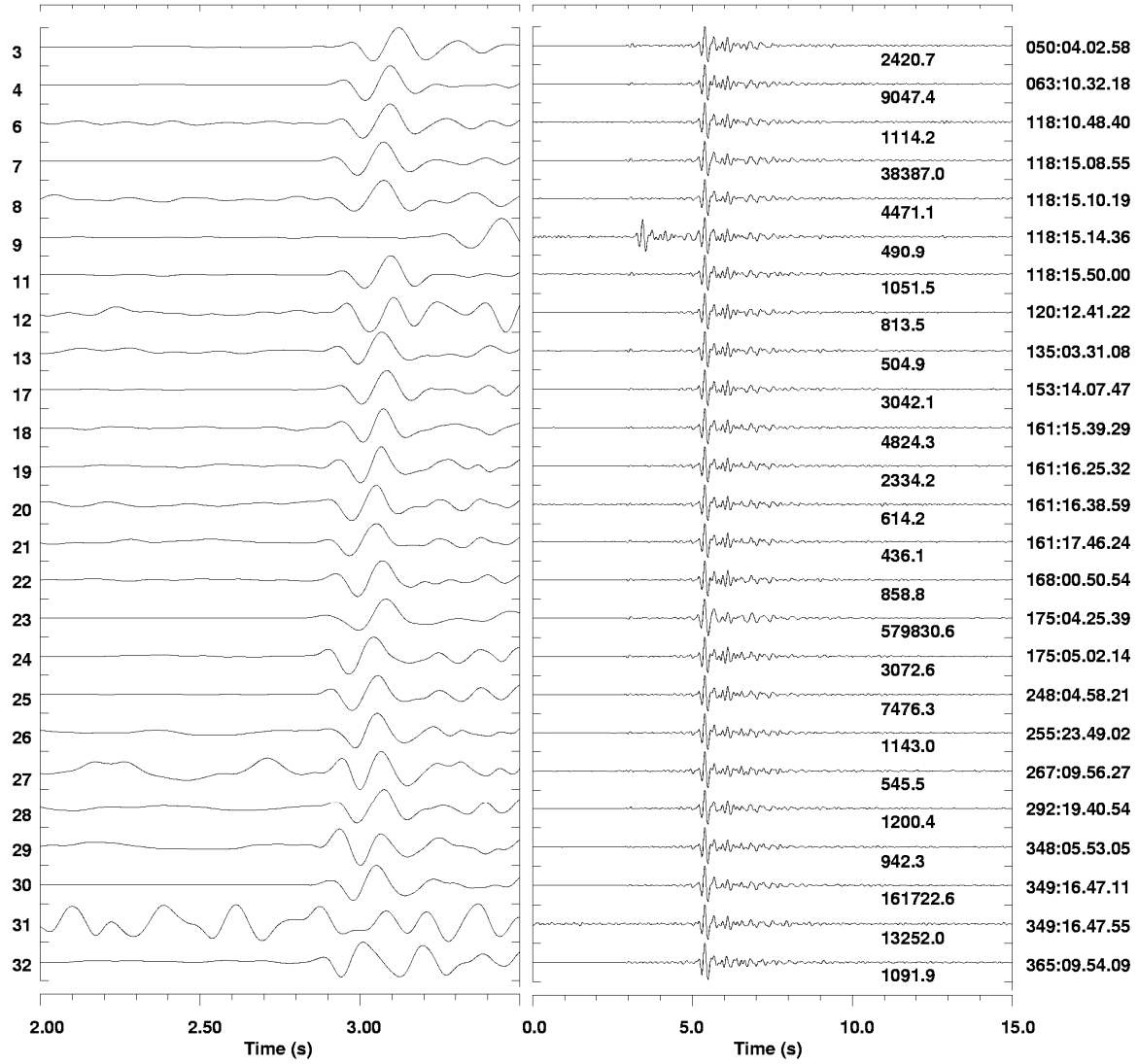

Figure 18. Waveforms recorded at the STOK station aligned with respect to the maximum correlation coefficient in a window following the S wave. The right panel shows a 15 s time segment, the left panel shows a 1.5 s zoom on the P arrivals. Waveforms are bandpass filtered between 2-8 Hz. Detection nr. 9 shows two events in rapid succession of each other. The arrival seen in the left panel for this detection is the S arrival for the first event.

Variations in the time difference between correlations at two arrays for different events (table 4 of paper 7) may be due to either varying locations, waveform

dissimilarity or timing errors at the recording stations. As discussed in paper 7, the most likely cause for varying differential arrival times for the Rana events are differences in location among the events. Figure 18 shows waveforms for 25 of the 32 events recorded at STOK, aligned with respect to the greatest correlation coefficient for a window following the S-waves. The left panel is zoomed in on the P waves and shows that these arrive within 0.05 s, indicating a maximum distance at the order of 500 m between the events.

We see from paper 7 that in the case where high-quality master events are available, waveform correlation detectors can increase the detection threshold at array stations by at least one order of magnitude. In addition, the correlation detectors provide the opportunity of associating events with a known source, thereby saving analyst time. The combination of correlation detectors and traditional STA/LTA detectors therefore provides an efficient basis for seismic monitoring, especially in a place like Norway with a high number of explosions.

4. Conclusions

The work presented in this thesis covers a wide range of topics, which have been separated into two main parts associated with direct seismic hazard assessment and seismotectonics. The following conclusions can be drawn based on this work:

- The city of Istanbul is under a significant seismic hazard due to the short distance to the NAF in the Marmara Sea, which is likely to break in a large earthquake in the near future. A high level of knowledge about the tectonics of the region makes scenario based ground motion modelling a feasible approach for seismic hazard assessment providing more reliable results than probabilistic methodologies.

- A M=7.5 earthquake in the Marmara Sea will have a significant effect on the city of Istanbul leading to ground accelerations at the level of 0.5g and ground velocities above 50 cm/s at bedrock level in the southern part of the city.

- Simulated ground motion is sensitive to the input source and attenuation parameters. The most important parameters in terms of ground motion level are rise time, rupture velocity, rupture initiation point and stress drop. The stress drop and attenuation have their main effect on the high-frequency ground motion whereas rupture velocity and rise time mainly affect the lower frequencies.

- The variability of simulated response spectra for varying source and attenuation parameters is strongly frequency dependent, especially for the acceleration response spectra which show large variability for f>5Hz. On the contrary, velocity response spectra show little variation underlining the strength of ground motion modelling despite the uncertainties involved.

- Attenuation of seismic waves plays an important role for the obtained hazard levels, especially for the PSHA. We provide a new attenuation relation based

on the background seismicity for the Marmara Sea region, which shows results in general agreement with previously used relationships.

- Local site effects are another important issue in seismic hazard assessment. In the case of the Ataköy district in southwestern Istanbul, significant site amplifications are expected. For alluvial deposits, amplification up to a factor of 2 is expected at frequencies around 1Hz and 3-6Hz. For the Bakirköy and Güngören formations, amplifications at a lower level are expected around 1Hz.

- The December 26, 2004 Sumatra-Andaman earthquake was associated with significant ground shaking, which may have caused severe damage in northern Sumatra and the neighbouring islands before the tsunami hit. For Banda Aceh, modelled ground velocities up to 60 cm/s at bedrock level can explain the reported ground shaking intensities up to IX when adding local site effects.

- The future hazard in the Sumatra region is associated with strong earthquakes along the plate interface in addition to a possible large strike-slip earthquake along the Great Sumatran Fault.

- The Norwegian area represents a diverse tectonic region covering both an active plate boundary and more stable continental interiors. This is reflected in the seismicity, which is concentrated in a number of regions of varying origin.

- The JMFZ located along the mid-Atlantic ridge has experienced several M=6+ earthquakes through history. Recently mapped bathymetry and high-quality recordings of a M=6 earthquake and its aftershocks have made direct correlation of an earthquake to a specific fault structure possible for the first time in Norway.

- The April 14, 2004 Jan Mayen earthquake ruptured a 10 km segment of the Koksneset fault. Redistribution of stresses due to the earthquake lead to the reactivation of NE-SW oriented structures in the JMP, probably through normal or oblique normal faulting.

- The Skagerrak region south of Norway is an active region within the Eurasian plate. Activity here is mainly associated with a previously unknown N-S oriented graben structure named the Langust fault zone. In addition, the STZ shows signs of activity also in this region.

- Recent recording from a new local network in the Rana region confirms the finding of Hicks et al. (2000b), that earthquake activity in the region is clustered and not associated with the Båsmoen fault. However, further processing is needed before detailed conclusions can be drawn based on the local data set.

- Event detection based on waveform cross-correlation of array data decreases the detection threshold significantly in comparison to traditional STA/LTA detectors applied to the array data. Such detectors can potentially save significant analyst time by associating events to known sources automatically.

A number of questions still remain to be answered, which provide interesting topics for future studies. Among these are modelling of ground motion from individual ruptures of the NAF segments in the Marmara Sea, implementation of local site effects in the ground motion methodologies, modelling of ground motion caused by a large earthquake along the Great Sumatran Fault, further investigations of the activity on the Koksneset fault and in the JMP including data from the newly installed station in northern Jan Mayen and joining the large amount of data becoming available from the temporary Rana network in a seismotectonic study for the region. Such studies will hopefully take advantage of the results presented in this thesis.

In the present thesis, the challenges related to seismic hazard assessment in both low and high seismicity regions have been addressed. It became clear that different regions require different methodologies depending upon the existing level of knowledge. The results of the individual studies reveal new clues about the studied regions, and hence, hopefully, serve as a step forward towards a better understanding of the seismic hazard.

References

Aksu, A.E., Calon, T., Hiscott, R.N. and Yasar, D., 2000. Anatomy of the North Anatolian Fault Zone in the Marmara Sea, Western Turkey: Extensional Basins Above a Continental Transform, GSA Today, 10, 6, 3-7.

Ambraseys, N.N., 2005. Revesion of the long-term seismicity of the greater Marmara Sea region, progress report, RELIEF project, 18pp.

Ambraseys, N.N. and Finkel, C.F., 1995. The Seismicity of Turkey and Adjacent Areas: A Historical Review 1500-1800, Eren Yayincilik ve Kitapcilik Ltd. Sti., Istanbul, 240pp.

Ambraseys, N.N. and Jackson, J.A., 2000. Seismicity of the Sea of Marmara (Turkey) since 1500, Geophysical Journal International, 141, F1-F6.

Ambraseys, N.N., Simpson, K.A. and Bommer, J.J., 1996. Prediction of horizontal response spectra in Europe, Earthquake Engineering and Structural Dynamics, 25, 371-400.

Ammon, C.J., Ji, C., Thio, H-K., Robinson, D., Ni, S., Hjorleifsdottir, V., Kanamori, H., Lay, T., Das, S., Helmberger, D., Ichinose, G., Polet, J., and Wald, D., 2005. Rupture process of the 2004 Sumatra-Andaman earthquake, Science, Vol.308, 1133-1139.

Ansal, A., Laue, J., Buchheister, J., Erdik, M., Springman, S.M., Studer, J. and Koksal, D.,2004. Site characterization and site amplification for a seismic microzonation study in Turkey, Proceedings of the 11th Intl. Conf. on Soil Dyn. & Earthquake Engng. (11th ICSDEE) & the 3rd Intl. Conf. on Earthquake Geotech. Engng. (3rd ICEGE), January 7-9, Berkeley, CA, pp. 53-60.

Armijo, R., Meyer, B., Navarro, S., King, G. and Barka, A., 2002. Asymmetric spli partitioning in the Sea of Marmara pull-apart: a clue to propagation processes of the North Anatolian Fault?, Terra Nova, 14, 80-86.

Armijo, R., Pondard, N., Meyer, B., Ucarkus, G., Mercier de Lepinay, B., Malavieille, J., Dominguez, S., Gustcher, M.-A., Schmidt, S., Bech, C., Cagatay, N., Cakir, Z., Imren, C., Eris, K., Natalin, B., Özalaybay, S., Tolun, L., Lefevre, I., Seeber, L., Garperini, L., Rangin, C., Emre, O. and Sarikavak, K., 2005. Submarine fault scarps in the Sea of Marmara pull-apart (North Anatolian Fault): Implications for seismic hazard in Istanbul, Geochemestry, Geophysics, Geosystems, 6, Q06009, doi:10.1029/2004GC000896.

Atkinson, G. M., and W. Silva, 2000. Stochastic Modeling of California Ground Motion, Bulletin of the Seismological Society of America, 90, 255-274.

Atakan, K., Karpuz, M.R. and Dahl, S.O., 1996. Importance of geological data in probabilistic seismic hazard assessments: a case study from Etne, western Norway, in Schenk, V. (ed.), Seismic Hazard and Risk, 169-198.

Atakan, K., Lindholm, C.D. and Havskov, J., 1994. Earthquake swarms in Steigen, northern Norway: an unusual example of intraplate seismicity, Terra Nova, 6, 180-194.

Atakan, K., Ojeda, A., Megraoui, M., Barka, A.A., Erdik, M. and Bodare, A., 2002. Seismic Hazard in Istanbul following the 17 August 1999 Izmit and 12 November 1999 Düzce earthquakes, Bulletin of the Seismological Society of America, 92, 1, 466-482.

Barka, A.A. and Kadinsky-Cade, K., 1988. Strike-slip fault geometry in Turkey and its influence on earthquake activity, Tectonics, 7, 3, 663-684.

Barka, A., Akyüz, H.S., Altunel, E., Sunal, G., Cakir, Z., Dikbas, A., Yerli, B., Armijo, R., Meyer, B., de Chabalier, J.B., Rockwell, T., Dolan, J.R., Hartleb, R. Dawson, T., Christofferson, S., Tucker, A., Fumal, T., Langridge, R., Stenner, H., Lettis, W., Bachhuber, J. and Page, W. (2002). The Surface Rupture and Slip Distribution of the 17 August 1999 Izmit Earthquake (M 7.4), North Anatolian Fault, Bulletin of the Seismological Society of America, 92, 1, 43-60.

Bilham, R., 2005. A flying start, then a slow slip. Science, Vol.308, 1126-1127.

Birgören, G., Özel, O., Fahjan, Y. and Erdik, M., 2004. Determination of site effects in Istanbul area using a small earthquake record of the dense strong motion network, XXIX General Assembly of the European Seismological Commision, Potsdam, Germany, poster no. 249.

Boettcher, M.S. and Jordan, T.H. (2004), Earthquake scaling relations for mid-ocean ridge transform faults, Journal of Geophysical Research, 109, B12302, doi:10.1029/2004JB003110.

Boettcher, M.S. (2005), Slip on Ridge Transform Faults: Insights from Earthquakes and Laboratory Experiments, Ph.D. thesis, Massachusetts Institute of Technology and Woods Hole Oceanographic Institution.

Bonnefoy-Claudet, S., Cornou, C., Kristek, J., Ohrnberger, M, Wathelet, M., Bard, P.-Y., Moczo, P., Faeh, D. & Cotton, F., 2004. Simulation of seismic ambient noise: I. Results of H/V and array techniques on canonical models, Proceedings of the 13th World Conference on Earthquake Engineering, Vancouver, Canada, 1-6 August, 2004, paper no. 1120.

Boore, D. M., W. B. Joyner and T. E. Fumal, 1997. Equations for Estimating Horizontal Response Spectra and Peak Acceleration from Western North American Earthquakes: A summary of Recent Work. Seismological Research Letters, 68, 1, 128-153.

Bungum, H., Hokland, B., Husebye, E.S. and Ringdal, F., 1979. An exceptional intraplate earthquake sequence in Meløy, northern Norway, Nature, 280, 32-35.

Bungum, H., Alsaker, A., Kvamme, L.B. and Hansen, R.A., 1991. Seismicity and Seismotectonics of Norway and Nearby Continental Shelf Areas, Journal of Geophysical Research, 96, B2, 2249-2265.

Bungum, H., Lindholm, C.D., Dahle, A., Woo, G., Nadim, F., Holme, J.K., Gudmestad, O.T., Hagberg, T. and Karthigeyan, K., 2000. New Seismic Zoning Maps for Norway, the North Sea, and the United Kingdom, Seismological Research Letters, 71, 6, 687-697.

Bungum, H. and Selnes, P.B., 1988. Earthquake Loading on the Norwegian Continental Shelf – Summary report, Norwegian Geotechnican Institute and NORSAR, 38pp.

Campbell, K.W., 1997. Empirical near source attenuation relationship for horizontal and vertical components of peak ground acceleration, peak ground velocity, and pseudo absolute acceleration response spectra, Seismological Research Letters, 68, 1, 154-179.

Dehls, J.F., Olesen, O., Bungum, H., Hicks, E.C., Lindholm, C.D. and Riis, F., 2000. Neotectonic map: Norway and adjacent areas. Geological Survey of Norway.

DeMets, C., Gordon, R.G., Argus, D.F. and Stein, S. (1990), Current plate motions, Geophysical Journal International, 101, 425-478.

DeMets, C., Gordon, R.G., Argus, D.F. and Stein, S. (1994), Effect of recent revisions to the geomagnetic reversal time scale on estimates of current plate motions, Geophysical Research Letters, 21, 2191-2194.

Doré, A.G. and Gage, M.S., 1987. Crustal alignments and sedimentary domains in the evolution of the North Sea, North-east Atlantic Margin and Barents Shelf, in: Brooks, J. and Glennie, K. (Eds.). Petroleum Geology of North West Europe, Graham & Trotman, pp. 1131-1148.

Erdik, M., Fahjan, Y., Özel, O., Alcik, H., Mert, A., and Gül, M. 2003. Istanbul Earthquake Rapid Response and the Early Warning System. Bulletin of Earthquake Engineering, 1, 157-163.

Erdik, M., Demircioglu, M., Sesetyan, K., Durukal, E. And Siyahi, B., 2004. Earthquake hazard in Marmara Region, Turkey, Soil Dynamics and Earthquake Engineering, 24, 605-631.

Ergün, M. and Özel, E., 1995. Structural relationship between the Sea of Marmara Basin and the North Anatolian Fault Zone, Terra Nova, 7, 278-288.

Eyidogan, H., Ecevitoglu, B. and Caglar, I., 2000 (in Turkish). Bakirköy Ilcesi 1. etap (Bakirköy Ataköy) yerlesim alanlarinin jeolojik yapi ve depremsellik etüdü projesi, Internal Report, part 6, TC. Bakirköy Belediyesi and ITÜ Gelistirme Vakfi. 55 p.

Eyidogan, H., Güclü, U., Utku, Z. and Degirmenci, E., 1991. Türkiye büyük depremleri makro-sismik rehberi (1900-1988) (in Turkish), Istanbul Technical University, Faculty of Mining, Department of Geological Engineering. Kurtis Matbaasi, Istanbul, 198pp.

Fejerskov, M. and Lindholm, C., 2000. Crustal stress in and around Norway: an evaluation of stress-generating mechanisms, in: Nøttvedt, A. et al. (Eds.). Dynamics of the Norwegian Margin, Geological Society of London, Special Publications, 167, 451-467.

Geller, R.J. and Mueller, C.S., 1980. Four Similar Earthquakes in Central California, Geophysical Research Letters, 7 (10), 821-824.

Gerstenberger, M., Wiemer, S. and Jones, L., 2004. Real-time Forecasts of Tomorrow's Earthquakes in California: A New Mapping Tool, U.S. Geological Survey, open-file report 2004-1390, 39pp.

Gibbons, S. and Ringdal, F., 2004. A waveform correlation procedure for detecting decoupled chemical explosions, NORSAR Scientific Report: Semiannual Technical Summary No. 2 – 2004, NORSAR, Kjeller, Norway, pp. 41-50.

Gibbons, S. and Ringdal, F., 2006. The detection of low magnitude seismic events using array-based waveform correlation, Geophysical Journal International, 165, 149-166, doi:10.1111/j.1365-246X.2006.02865.x.

Gregersen, S., 1979. Earthquakes in the Skagerrak recorded at small distances, Bulletin of the Geological Society of Denmark, vol. 28, 5-9.

Gregersen, S., 1992. Crustal stress regime in Fennoscandia from focal mechanisms, Journal of Geophysical Research, 97, 11821-11827.

Gregersen, S. and Arvidsson, R., 1992. Atlas Map 5, Focal Mechanisms. In: D. Blundell, R. Freeman and S. Mueller (Editors), A continent Revealed: The European Geotraverse. Cambridge University Press.

Gregersen, S., Hjelme, J. And Hjortenberg, E., 1996a. Earthquakes in Denmark, Bulletin of the Geological Society of Denmark, vol. 44, 115-127.

Gregersen, S., Leth, J., Lind, G. And Lykke-Andersen, H., 1996b. Earthquake activity and its relationship with geologically recent motion in Denmark, Tectonophysics, 257, 265-273.

Grønlie, G., Chapman, M. and Talwani, M., 1979. Jan Mayen Ridge and Iceland Plateau: origin and evolution, Norsk Polarinstitutt Skrifter, 170, 25-47.

GSHAP, 1999. GSHAP Summary Volume, Annali di Geofisica, 1999.

Haase, K.M. and Devey, C.W. (1994), The petrology and geochemistry of Vesteris Seamount, Greenland Basin – an intraplate alkaline volcano of non-plume origin, Journal of Petrology, 35, 295-328.

Haase, K.M., Devey, C.W., Mertz, D.F., Stoffers, P. and Garbe-Schönberg, D., 1996. Geochemistry of lavas from Mohns Ridge, Norwegian-Greenland Sea: implications for melting conditions and magma sources near Jan Mayen, Contributions to Mineralogy Petrology, 123, 223-237.

Harris, D.B., 1991. A waveform correlation method for identifying quarry explosions, Bull. Seism. Soc. Am., 81, 2395-2481.Riviére-Barbier, F. and Grant, L.T., 1993. Identification and Location of Closely Spaced Mining Events, Bulletin of the Seismological Society of America, 83, 1527-1546.

Havskov, J. and Atakan, K., 1991. Seismicity and volcanism of Jan Mayen Island, Terra Nova, 3, 517-526.

Hicks, E.C., 1996. Crustal Stresses in Norway and Surrounding Areas as Derived From Earthquake Focal Mechanism Solutions and In-Situ Stress Measurements, Cand. Scient. Thesis, Department of Geology, University of Oslo.

Hicks, E.C., Bungum, H. and Lindholm, C., 2000a. Stress inversion of earthquake focal mechanism solutions from onshore and offshore Norway, Norsk Geologisk Tidsskrift, 80, 235-250.

Hicks, E.C., Bungum, H. and Lindholm, C., 2000b. Seismic activity, inferred crustal stresses and seismotectonics in the Rana region, Northern Norway, Quarternary Science Reviews, 19, 1423-1436.

Hubert-Ferrari, A., Barka, A., Jacques, E., Nalbant, S.S., Meyer, B., Armijo, R., Tapponnier, P. and King, G.C.P. (2000). Seismic hazard in the Marmara Sea region following the 17 August 1999 Izmit earthquake, Nature, 404, 269-273.

IBB. 2003. Earthquake Master Plan for Istanbul. Metropolitan Municipality of Istanbul, Turkey. 1300p.

Imren, C., Le Pichon, X., Rangin, C., Demirbag, E., Ecevitoglu, B. and Görür, N., 2001. The North Anatolian Fault within the Sea of Marmara: a new interpretation based on multi-channel seismic and multi-beam bathymetry data, Earth and Planetary Science Letters, 186, 143-158.

Imsland, P., 1978. The geology of the volcanic island Jan Mayen Arctic Ocean, Nordic Volcanological Institute Research Papers, 7812, 1-74.

Imsland, P., 1986. The volcanic eruption on Jan Mayen, January 1985: Interaction between a volcanic island and a fracture zone, Journal of Volcanology and Geothermal Research, 28, 45-53.

Israelsson, H., 1990. Correlation of waveforms from closely spaced regional events, Bulletin of the Seismological Society of America, 80, 6, 2177-2193.

Japan International Cooperation Agency (JICA) 2004. Country Strategy Paper for Natural Disasters in Turkey, JICA-Report, Turkiye Cumhuriyeti Icisleri Bakanligi, Ankara, July 2004, 154p.

Ji, C., 2005. Preliminary rupture model of the December 26, 2005 Sumatra earthquake, available at http://neic.usgs.gov/neis/eq_depot/2004/eq_041226/neic_slav_ff.html.

Kijko, A. and Sellevoll, M.A., 1990. Estimation of Earthquake Hazard Paramerers for Incomplete and Uncertain Data Files, Natural Hazards, 3, 1-13.

Kodaira, S., Mjelde, R., Gunnarsson, K., Shiobara, H. And Shimamura, H., 1998. Evolution of oceanic crust on the Kolbeinsey Ridge, north of Iceland, over the past 22 Myr, Terra Nova, 10, 27-31.

Kreemer, C., Holt, W.E., and Haines, A.J. (2003), An integrated global model of present-day plate motions and plate boundary deformation, Geophysical Journal International, 154, 8-34.

Lay, T., Kanamori, H., Ammon, C., Nettles, M., Ward, S.N., Aster, R.C., Beck, S.L., Bilek, S.L., Brudzinski,M.R., Butler, R., DeShon, H.R., Ekström, G., Satake, K., Sipkin, S., 2005. The great Sumatra-Andaman earthquake of December 26, 2004. Science, Vol.308, 1127-1133.

Lay, T. and Wallace, T., 1995. Modern Global Seismology, Academic Press, San Diego.

Le Pichon, X., Sengör, A.M.C., Demirbag, E., Rangin, C., Imren, C., Armijo, R., Görür, N., Cagatay, N., Mercier de Lepinay, B., Meyer, B., Saatcilar, R. and Tok, B., 2001. The active Main Marmara Fault, Earth and Planetary Science Letters, 192, 595-616.

Le Pichon, X., Chamot-Rooke, N., Rangin, C. and Sengör, A.M.C., 2003. The North Anatolian Fault in the Sea of Marmara, Journal of Geophysical Research, 108, B4, 2179, doi:10.1029/2002JB001862.

Lermo, J. & Chávez-García, F.J., 1993. Site effect evaluation using spectral ratios with only one station. Bulletin of the Seismological Society of America., 83, 1574-1594.

Lie, J.E. and Andersson, M., 1998. The deep-seismic image of the crustal structure of the Tornquist Zone beneath the Skagerrak Sea, Northwestern Europe, Tectonophysics, 287, 139-155.

Lindholm, C. and Bungum, H., 2000. Probabilistic seismic hazard: a review of the seismological frame of reference with examples from Norway, Soil Dynamics and Earthquake Engineering, 20, 27-38.

McCaffrey, R., Zwick, P.C., Bock, Y., Prawiradirdjo, L., Genrich, J.F., Stewens, C.W., Puntodewo, S.S.O., and Subarya, C., 2000. Strain partitioning during oblique plate convergence in northern Sumatra: Geodetic and seismologic constraints and numerical modeling. Journal of Geophysical Research, Vol.105, No.B12, 28,363-28,376.

McClusky, S., Balassanian, S., Barka, A., Bemir, C., Ergintav, S., Georgiev, I., Gurkan, O., Hamburger, M., Hurst, K., Kahle, H., Kastens, K., Kekelidze, G., King, R., Kotzev, V., Lenk, O., Mahmoud, S., Mishin, A., Nadariva, M., Ouzounis, A., Paradissis, D., Peter, Y., Prilepin, M., Reilinger, R., Sanli, I., Seeger, H., Tealeb, A., Toksöz, M.N. and Veis, G., 2000. Global Positioning System constraints on plate kinematics and dynamics in the eastern Mediterranean and Caucasus, Journal of Geophysical Research, 105, B3, 5695-5719.

McClousky, J., Nalbant, S.S., and Stacy, S. 2005. Earthquake risk from co-seismic stress. Nature, Vol.434, 291.

Menke, W., 2001. Using Waveform Similarity to Constrain Earthquake Locations, Bull. Seism. Soc. Am., 89, 4, 1143-1146.

Morgan, W.J., 1981. Hotspot tracks and the opening of the Atlantic and Indian Oceans. In: Emiliani, C. (Ed.), The oceanic lithosphere (The sea, vol. 7), Wiley and Sons, New York, 443-487.

Mosar, J., Eide, E.A., Osmundsen, P.T., Sommaruga, A. And Torsvik, T.H., 2002. Greenland – Norway separation: A geodynamic mode for the North Atlantic, Norwegian Journal of Geology, 82, 281-298.

Muir-Wood, R., 1989. The Scandinavian earthquakes of 22 December 1759 and 31 August, 1819, Disasters, 12, 223-236.

Nakamura, Y., 1989. A method for dynamic characteristics estimation of subsurface using microtremors on the ground surface. Q. Rep. Railway Tech. Res. Inst., 30, 1.

Nakamura, Y., 2000. Clear identification of fundamental idea of Nakamura's technique and its applications, proceedings of the 12th WCEE, New Zealand, paper no. 2656.

Oglesby, D.D., Mai, P.M., Atakan, K., Pantosti, D., and Pucci, S. 2005. Dynamic rupture in the presence of fault discontinuities: An application to the faults in the Marmara Sea. AGU Fall Meeting, San Francisco, USA, Dec.5-9, 2005.

Okay, A.I., Kaslilar-Özcan, A., Imren, C., Boztepe-Güney, A., Demirbag, E. and Kuscu, I., 2000. Active faults and evolving strike-slip basins in the Marmara Sea, northwest Turkey: a multichannel seismic reflection study, Tectonophysics, 321, 189-218.

Oprsal, I., Brokesova, J., Faeh, D., & Giardini, D., 2002. 3D Hybrid Ray-FD and WNFD Seismic Modeling For Simple Models Containing Complex Local Structures, Studia Geophysica et Geodaetica, 46, 711-730.

Oprsal, I. & Zahradnik, J., 2002. Three-dimensional finite difference method and hybrid modeling of earthquake ground motion, Journal of Geophysical Research, 107(B8), DOI 10.1029/2000JB000082.

Oprsal, I., Faeh, D., Mai, M. & Giardini, D., 2005. Deterministic earthquake scenario for the Basel area - Simulating strong motion and site effects for Basel, Switzerland, Journal of Geophysical Research, 110, doi:10.1029/2004JB003188.

Ortiz, M., and Bilham, R., 2003. Source are and rupture parameters of the 31 December 1881 MW=7.9 Car Nicobar earthquake estimated from tsunamis recorded in the Bay of Bengal. Journal of Geophysical Research, Vol.108, No.B4, 2215-2229.

Özbey, C., Sari, A., Manuel, L., Erdik, M. Fahjan, Y., 2004. An empirical attenuation relationship for Northwestern Turkey ground motion using a random effects approach, Soil Dynamics and Earthquake Engineering, 24, 115–125

Özel, O., Birgören, G., Alcik, H. 2005. Natural frequencies of the sedimentary cover in Istanbul from weakmotion records and microtremor measurements. Poster presentation, Seismological Society of Japan 2005 Fall Meeting, Sapporo, Japan.

Park, J., Anderson, K., Aster, R., Butler, R., Lay, T., and Simpson, D. 2005. Global Seismographic Network records the great Sumatra-Andaman earthquake. EOS, Vol.86, No.6, 57-64.

Parke, J.R., Minshull, T.A., White, R.S., McKenzie, D., Kuscu, I., Bull, J.M., Görür, N. and Sengör, C., 1999. Active faults in the Sea of Marmara, western Turkey, imaged by seismic reflection profiles, Terra Nova, 11, 223-227.

Parsons, T., 2004. Recalculated probability of M ≥ 7 earthquakes beneath the Sea of Marmara, Turkey, Journal of Geophysical Research, 109, B05304, doi: 10.1029/2003JB002667.

Pedersen R.B. Svellingen, W. and Hellevang, B. (in prep), The submarine geology of the Jan Mayen region: A unique example of ridge-transform-micro continent interaction. (manuscript in prep.).

Petersen, M.D., Dewey, J., Hartzell, S., Mueller, C., Harmsen, S., Frankel, A.D. and Rukstales, K., 2004. Probabilistic seismic hazard analysis for Sumatra, Indonesia and across the Southern Malaysian Peninsula, Tectonophysics, 390, 141-158.

Prawirodirdjo, L., Bock, Y., McCaffrey, R., Genrich, J., Calais, E., Stevens, C., Puntodewo, S.S.O., Subarya, C., Rais, J., Zwick, P., and Fauzi, 1997. Geodetic observations of interseismic strain segmentation at the Sumatra subduction zone. Geophysical Research Letters, Vol.24, No.21, 2601-2604.

Pulido, N., Ojeda, A., Atakan, K. & Kubo, T., 2004. Strong ground motion estimation in the Marmara Sea region (Turkey) based on a scenario earthquake. Tectonophysics, 391, 357-374.

Reinecker, J., Heidbach, O., Tingay, M., Sperner, B. & Müller, B. (2005): The release 2005 of the World Stress Map (available online at www.world-stress-map.org).

Ringdal, F., Husebye, E.S., Bungum, H., Mykkeltveit, S. and Sandvin, O.A., 1982. Earthquake hazard offshore Norway, a study for the NTNF "Safety offshore" committee, NORSAR report, Kjeller, Norway.

Sadigh, K., Chang, C.-Y., Egan, J.A., Makdisi, F. and Youngs, R.R., 1997. Attenuation relationship for shallow crustal earthquakes based on California strong motion data, Seismological Research Letters, 68, 1, 180-189.

Sato, T., Kasahara, J., Taymaz, T., Ito, M., Kamimura, A., Hayakawa, T. and Tan, O., 2004. A study of microearthquake seismicity and focal mechanisms within the Sea of Marmara (NW Turkey) using ocean bottom seismometers (OBSs), Tectonophysics, 391, 303-314.

Schilling, J.-G., Zajac, M., Evans, R., Johnston, T., White, W., Devine, J.D. and Kingsley, R., 1983. Petrologic and geochemical variations along the Mid-Atlantic Ridge from 29°N to 73°N, American Journal of Science, 283, 510-586.

Scheck-Wenderoth, M. and Lamarche, J., 2005. Crustal memory and basin evolution in the Central European Basin System – new insights from a 3D structural model, Tectonophysics, 297, 143-165.

Schulte-Theis, H. and Joswig, M., 1993. Clustering and location of mining induced seismicity in the Ruhr Basic by automated Master Event Comparison based on Dynamic Waveform Matching (DWM), Computers and Geosciences, 91, 2, 233-241.

Sengör, A.M.C., Tüysüz, O., Imren, C., Sakinc, M., Eyidogan, H., Görür, N., Le Pichon, X. and Rangin, C., 2005. The North Anatolian Fault: A New Look, Annual Review of Earth and Planetary Sciences, 33, 37-112.

Simoes, M., Avouac, J.P., Cattin, R., and Henry, P. 2004. The Sumatra subduction zone: A case for a locked fault zone extending into mantle. Journal of Geophysical Research, Vol.109, No.B10402, 16p.

Singh, S.K., Ordaz, M., Lindholm, C.D. and Havskov, J., 1990. Seismic hazard in southern Norway, Seismo-series 46, Institute of Solid Earth Physics, University of Bergen, 33pp.

Siyako, M., Tanis, T. and Saroglu, F., 2000. Marmara Deniz aktif fay geometrisi. TÜBITAK Bilim Tek. Derg., 388, 66-71.

Somerville, P., Irikura, K., Graves, R., Sawada, S., Wald, D., Abrahamson, N., Iwasaki, Y., Kagawa, T., Smith, N. and Kowada, A., 1999. Characterizing Crustal Earthquake Slip Models for the Prediction of Strong Ground Motion, Seismological Research Letters, 70, 59-80.

Stein, S., and Okal, E.A. 2005. Speed and size of the Sumatra earthquake. Nature, Vol.434, 581-582.

Stevens, J., Rimer, N., Xu, H., Murphy, J., Barker, B., Gibbons, S., Lindholm, C., Ringdal, F., Kværna, T. and Kitov, I., 2004. Analysis and simulation of cavity-decoupled explosions, in Proceedings of the 26th Seismic Research Review, Orlando, Florida, September 2004. Trends in Nuclear Explosion Monitoring, pp. 495-502.

Straub, C., Kahle, H.-G. and Schindler, C., 1997. GPS and geologic estimates of the tectonic activity in the Marmara Sea region, NW Anatolia, Journal of Geophysical Research, 102, B12, 27587-27601.

Svellingen, W. (2004), Submarin vulkanisme i Jan Mayen området, M.Sc. thesis, Department of Earth Science, University of Bergen.

Svellingen, W. and Pedersen, R.B., 2003. Jan Mayen: a result of ridge – transform – micro-continent interaction, EGS-AGU-EUG Joint Assembly, Nice, France, 6-11 April, abstract #12993.

Sylvester, A.G. (1975), History and surveillance of volcanic activity on Jan Mayen island, Bulletin of Volcanology, 39, 1-23.

Talwani, M. and Eldholm, O., 1977. Evolution of the Norwegian-Greenland Sea, Geological Society of America Bulletin, 88, 969-999.

Vogt, P.G., Johnson, G.L. and Kristjansson, L., 1980. Morphology and Magnetic Anomalies North of Iceland, Journal of Geophysics, 47, 67-80.

Waldhauser, F. and Ellswoth, W.L., 2000. A Double-Difference Earthquake Location Algorithm: Method and Application to the Northern Hayward Fault, California, Bulletin of the Seismological Society of America, 90, 6, 1353-1368.

Wells, D.L. and Coppersmith, K.J. (1994), New empirical relationships among magnitude, rupture length, rupture area and surface displacement, Bulletin of the Seismological Society of America, 84, 974-1002.

Wilson, J., 1973. Mantle Plumes and Plate Motions, Tectonophysics, 19, 149-164.

Wong, H.K., Lüdmann, T., Ulug, A. and Görür, N., 1995. The Sea of Marmara: a plate boundary sea in an escape tectonic regime, Tectonophysics, 231-250.

Yagi, Y. 2004. Preliminary results of rupture process for 2004 off coast of Northern Sumatra giant earthquake, available at http://iisee.kenken.go.jp/staff/yagi/eq/Sumatra2004/Sumatra2004.html

Yaltirak, C., 2002. Tectonic evolution of the Marmara Sea and its surroundings, Marine Geology, 190, 493-529.

Yamanaka, Y. 2005. Source rupture process of the Dec.26, 2004 Sumatra-Andaman earthquake. EIC-Seismological Note No.161, ERI, Univ.of Tokyo, Japan, available at http://www.eri.u-tokyo.ac.jp/sanchu/Seismo_Note/2004/EIC161e.html